HUNG-CHUNG LEE

Ph. D.

AL AND ANALYTICAL STUDY OF
OF ENTRY ANGLE IN VORTEX
TEMPERATURE SEPARATION

is for the Degree of Ph. D.
HIGAN STATE UNIVERSITY
Bung-Chung Lee
1960

This is to certify that the

thesis entitled

EXPERIMENTAL AND ANALYTICAL STUDY OF INFLUENCE OF ENTRY ANGLE IN VORTEX FLOW TEMPERATURE SEPARATION

presented by

BUNG-CHUNG LEE

has been accepted towards fulfillment of the requirements for

Doctor of Philosophy degree in Mechanical Engineering

J. E. Lay
Major professor

Date August 17, 1960

O-169

EXPERIMENTAL AND ANALYTICAL STUDY OF INFLUENCE OF ENTRY ANGLE IN VORTEX FLOW TEMPERATURE SEPARATION

By

BUNG-CHUNG LEE

AN ABSTRACT

Submitted to the School for Advanced Graduate Studies
of Michigan State University of Agriculture and
Applied Science in partial fulfillment of
the requirements for the degree of

DOCTOR OF PHILOSOPHY

Department of Mechanical Engineering

1960

Approved J. S. Foy.

BUNG-CHUNG LEE

ABSTRACT

This thesis reports on a study of the entry angle in vortex flow temperature separation based on experimental studies conducted for the Office of Ordnance Research, United States Army. It gives the performance characteristics of a vortex tube with respect to a wide range of "entrance" angles, from 90° (tangential flow) to 15° (near axial flow). Heretofore, data of this nature have been entirely lacking in the literature of the Ranque-Hilsch effect.

An experimental investigation was conducted on both the uniflow and the counterflow type of vortex tube, with pressure, temperature and velocity traverses taken at different stations along the length of the tube. Data were taken for runs with entry angles of 90°, 75°, 60°, 45°, 30°, and 15° respectively. An analytical study was made in terms of the Helmholtz and Kelvin theorems on vorticity. Later a "circulation" is considered to be induced from a vortex filament coincident with the axis of the tube, but of variable strength along the tube. The experimental data are then compared with those obtained from the use of Biot-Savart law. This results in a simpler interpretation of the data, especially in relation to viscous effects. The experimental results show that the entry angle has a marked effect on the Hilsch effect.

EXPERIMENTAL AND ANALYTICAL STUDY OF INFLUENCE OF ENTRY ANGLE IN VORTEX FLOW TEMPERATURE SEPARATION

By

BUNG-CHUNG LEE

A THESIS

Submitted to the School for Advanced Graduate Studies
of Michigan State University of Agriculture and
Applied Science in partial fulfillment of
the requirements for the degree of

DOCTOR OF PHILOSOPHY

Department of Mechanical Engineering

1960

To my parents

VITA

Bung-Chung Lee

candidate for the degree of

Doctor of Philosophy

Final examination: August 17, 1960, 9:00 A. M., Room 301, Olds Hall

Dissertation: Experimental and Analytical Study of Influence of Entry Angle in Vortex Flow Temperature Separation

Outline of Studies

Major Subject: Mechanical Engineering
Minor Subject: Mathematics, Physical Chemistry

Biographical Items

Born: October 19, 1927, Peiping, China
Undergraduate Studies: National Taiwan University, Taipei, Taiwan, Republic of China, 1949-1952
Graduate Studies: Georgia Institute of Technology, 1954-1955; Michigan State University, 1956-1960

Experience: Junior Engineer, Taiwan Shipbuilding Corporation, Keelung, Taiwan, Republic of China, 1953-1954; Graduate Assistant in Mechanical Engineering, Michigan State University, 1956-1958. Research Assistant Instructor in Division of Engineering Research, Michigan State University, 1958-1960

Member of Pi Mu Epsilon

ACKNOWLEDGEMENT

The author wishes to express his most sincere appreciation of the following people:

Dr. Joachim E. Lay, for his suggestion of the subject of this investigation, for his kindly concern in its successful completion and for his helpful, considerate and understanding guidance throughout the entire course of this study;

Drs. Ralph M. Rotty, Rolland T. Hinkle, Charles P. Wells and Max T. Rogers for their apt guidance on the author's committee;

Professor Leonard C. Price, Dr. Louis L. Otto, Mr. John W. Hoffman for their administrative support;

Professor Ralph L. Vanderslice for his help in taking the pictures;

Mr. Don W. Seble for his technical assistance in the expeditious production of experimental equipment;

The Office of Ordnance Research, United States Army, Duke Station, Durham, North Carolina for sponsorship of this study;

The Division of Engineering Research, Michigan State University, for the part-time employment which made the pursuit of the degree financially possible.

TABLE OF CONTENTS

LIST OF FIGURES

LIST OF FIGURES (Cont.)

LIST OF FIGURES (Cont.)

NOMENCLATURE

Symbol Used

c_p, c_v	specific heats at constant pressure and constant volume
$\vec{F}$	body force (including gravity force)
F_x, F_y, F_z	components of body force along x-, y-, and z-directions
g	acceleration of gravity
H	total head
h	height
K	constant of irrotational flow
$\vec{l}$	length vector; also vortex filament
$\vec{n}$	unit normal vector
p	pressure
Q	heat
$\vec{q}$	velocity vector
q_x, q_y, q_z, q_l	velocity components along x-, y-, z-, and length directions
R	gas constant
$\vec{r}$	position vector
S	surface area
s	entropy
T	absolute temperature
t	time
v	specific volume
$\vec{v}$	viscous force vector per unit volume

NOMENCLATURE (Cont.)

Symbol Used	
w'	work done per unit mass and time against viscous stresses at surface of an element of fluid
x, y, z	coordinate axes
γ	ratio of specific heats at constant pressure and volume; also limit of quotient of the circulation along the contour of a mesh to the area of the mesh
Γ	circulation
ϵ	eddy diffusivity
μ	viscosity
ρ	density
σ	normal stress
τ	shear stress
ω	fluid rotation
$\vec{\Omega}$	vorticity

I. INTRODUCTION

The vortex, or Ranque-Hilsch tube is a remarkably uncomplicated device which simultaneously produces hot and cold streams from a single source of compressed gas. The device has no moving parts, but merely consists of a straight length of tubing with a tangential entry for the supply air, and a smaller tube for tapping off the cold stream that is produced (Figure 1), the hot stream leaving through the large tube.

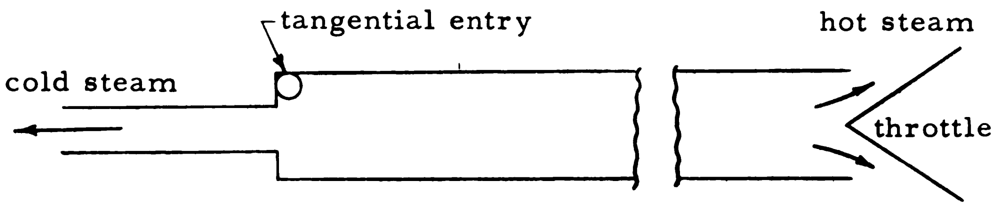

Figure 1. Simple Counterflow Vortex Tube

By throttling the far end of the larger tube, various proportions of hot and cold gas may be obtained with various degrees of temperature difference.

As a phenomenon, relatively little is known concerning it, except for its spectacular effect of producing hot and cold air simultaneously. Despite various hypotheses advanced, there is to date, no general agreement as to its theory of operation, and no way of predicting its performance. This is because the standard analytical treatment invariably leads to non-linear partial differential equations which are difficult to solve and which do not give a very realistic account of the effect of viscosity [7, 12, 13, 23].[1] Added to this is the fact that very meager experimental results are presently available to check the analytical assumptions made in theoretical papers. Both Ranque's and Hilsch's models were of small diameter (4 to 18 mm tubes with 2 to 7 mm orifices) wherein fairly impressive effects were obtained with relatively low or moderate supply pressures. Such small-size models, however, are not suitable for any systematic experimental study of the vortex phenomenon, since they do not lend themselves to any velocity, pressure or temperature traverses. Recently, large models have been designed [9, 20], but so far, none have incorporated a variable entry angle. The work reported here attempts to determine the influence of the entry angle by incorporating six different inlet angles in the design. This is an extension of the study first presented at the 1958 annual and semi-annual meetings of the A. S. M. E. [20]. The attention, however, is focussed on the influence of the entry angle, since this aspect of the vortex phenomenon has not yet been described in the literature.

---

[1] Numbers in brackets designate bibliography at the end of the thesis.

EXPERIMENTAL PROGRAM

Apparatus: The goal of the test program is to study the influence of entry angle in vortex flow temperature separation. In order to achieve this purpose, the temperature and pressure must be measured inside the vortex tube without causing major disturbances. Both Ranque's and Hilsch's original size model (4 mm to 18 mm tubes with 2 mm to 7 mm orifices) are unsuitable for gathering such information, and large size models must be considered. Recently large size models have been designed and put into operation. This program is an extension of the work that was first presented at the 1958 annual and semi-annual meetings of the A. S. M. E. [20]. Thus, the same size (2 in. inside diameter) lucite tube design (shown in Figure 2) was adopted in this program. To study the influence of the entry angle on the performance of the vortex tube, a series of center blocks were designed, incorporating entrance angles of 90° (tangential), 75°, 60°, 45°, 30° and 15°(near axial). The variation of the entry angle may be seen in Figure 3 which is a preliminary version of the actual test installation. The full size entry blocks for the test installation are shown in Figure 4. Corresponding to each entry angle, a run was made using compressed air of the small inlet pressure throughout, with pressure and temperature traverses systematically taken at six stations (Figure 5) along the vortex tube. An adjustable cone-shape valve (Figure 6) which can move in and out to regulate the flow is installed at the end of the vortex tube. Both the uniflow and counterflow types of vortex tubes were used (Figures 7 and 8) in this program.

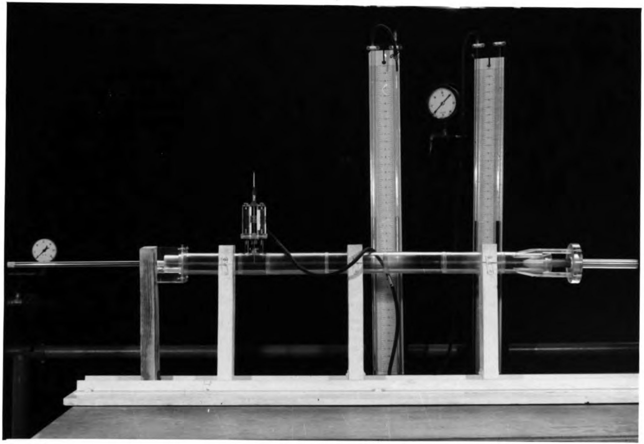

Figure 2. Vortex Tube Design

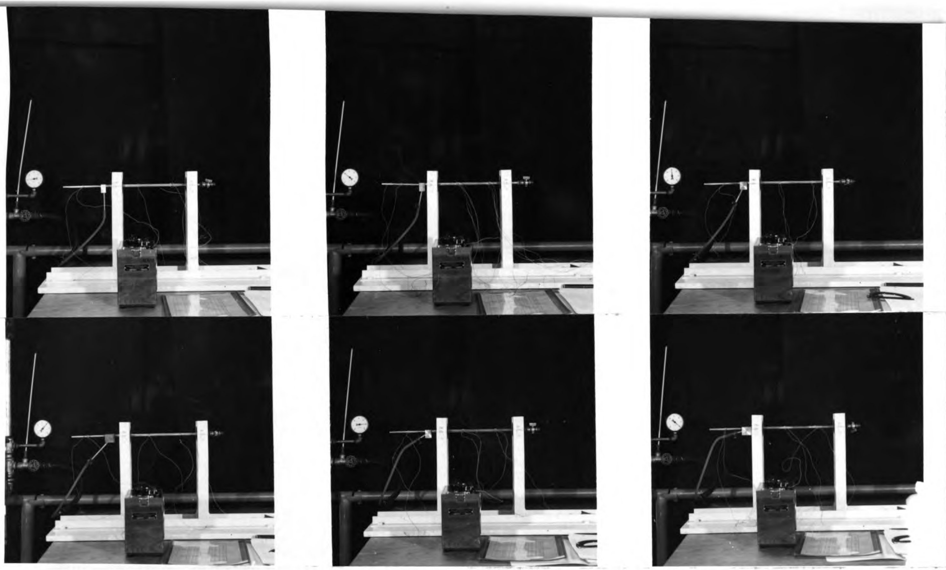

Figure 3. Preliminary Version of Vortex Tube with Variable Entry Angle

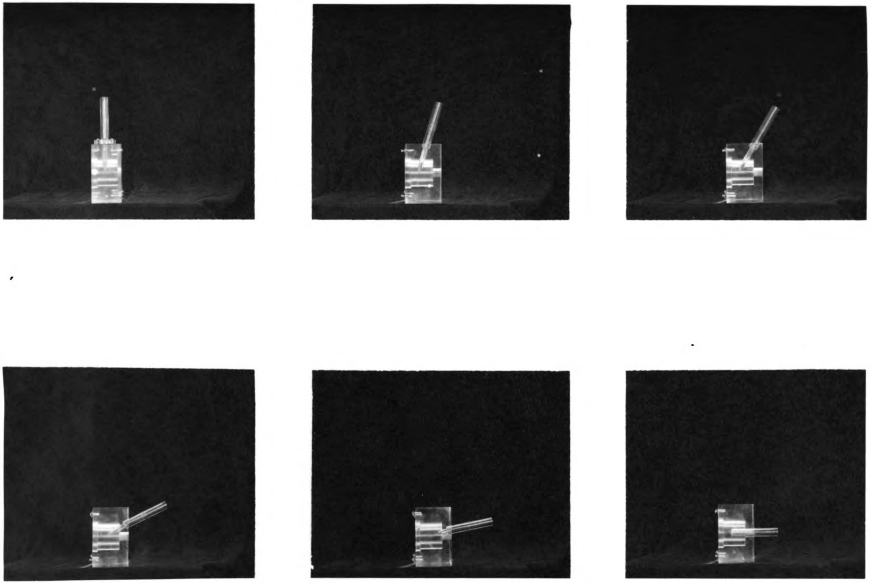

Figure 4. Full size entry angle block incorporating different entry angles.

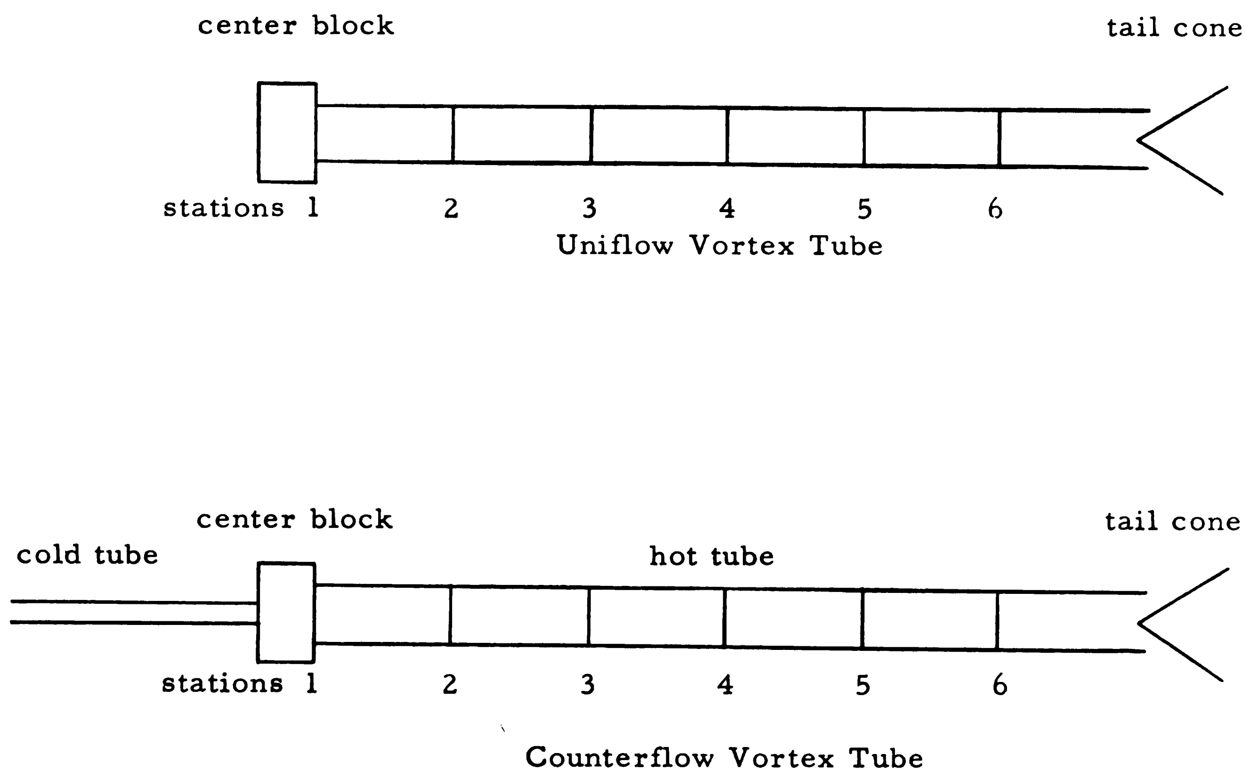

Figure 5. Locations of traverse stations.

Figure 6. Adjustable Cone-Shape Valve

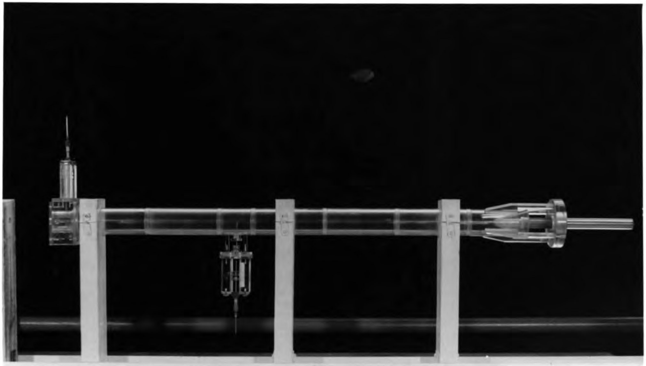

Figure 7. Uniflow Type of Vortex Tube

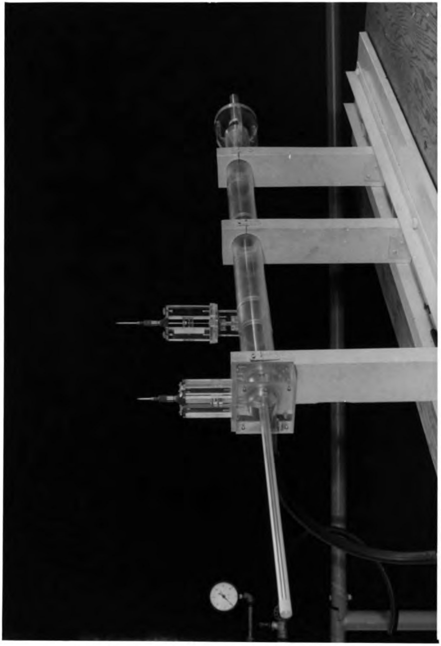

Figure 8. Counterflow Type of Vortex Tube

Instrumentation: In this test program, the instrumentation has been carefully designed to avoid causing major disturbances in the flow field. It is described in the following:

Probe assembly (Figure 9): It can be inserted at any station along the length of the vortex tube, and constructed in such a way that a hypodermic needle probe may be raised, lowered, or completely revolved within the flow field. The hypodermic needle probe is raised or lowered by means of a Brown and Sharpe 605 depth gage and slider and bearing assembly which is mounted on a stand. This stand is itself clamped by means of adjusting screws to another stand, with the latter being glued in place to the probe tube. Thus, the hypodermic needle is free to move to any radial position within the vortex tube, and it may also be revolved so as to be sensitive to direction as well as to magnitude of velocities.

Pressure probes: They consist of a static pressure probe, which is simply a stainless steel hypodermic tubing (#18 gage) well polished and open at the end, and of a total pressure probe. The static pressure probe is always inserted in such a way that it is perpendicular to the direction of flow. The total pressure probe is more elaborate, but essentially, it consists of a stainless steel hypodermic tube of similar size as the one for static pressure measurement, except that the open end is soldered closed, square cut, and polished. Near the tip of this hypodermic needle, a small hole is drilled. This opening, being always in the direct line of flow (since the axis of the tube is perpendicular to the line of flow) serves as an impact tube for the measurement of total pressure.

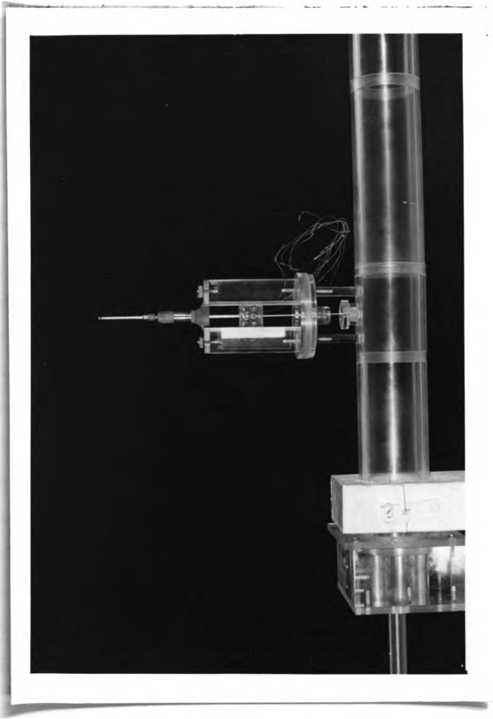

Figure 9. Probe Assembly

Temperature probe: It consists of a stainless steel hypodermic tube of similar size (#18 gage) as those used for the pressure probes; however, with two dissimilar but insulated leads (copper and constantan) inserted through it. The ends of the leads are fused together by an acetylene torch, then pulled back close to the end of the tube to make the assembly compact. Since all probes had to be kept as minute as possible so as not to disturb the flow field, no further elaboration (such as shielding for radiation, etc.) was induced in the manufacture of the probes.

The flow diagram of compressed air is shown in Figure 10. Compressed air is supplied by the Mechanical Engineering Laboratory Joy single cylinder air compressor to a storage tank, then passed through an air strainer, pressure regulator and an orifice, and finally transmitted by a simple flexible rubber hose into the vortex tube. Pressure gage #1 is accompanied by a regulator to check the pipe pressure; pressure gage #2 and thermometer are used to record the pressure and temperature respectively at the entrance to the vortex tube. A water or mercury manometer is connected before and after the 1/2 in. diameter orifice plate to measure the air flow.

Experimental procedure: Since particular interest is focussed on the influence of "entry angle," a certain reference datum is chosen in order to make the comparison of the experimental results. This is done as follows. First set up the counterflow vortex tube with a 90° entry angle

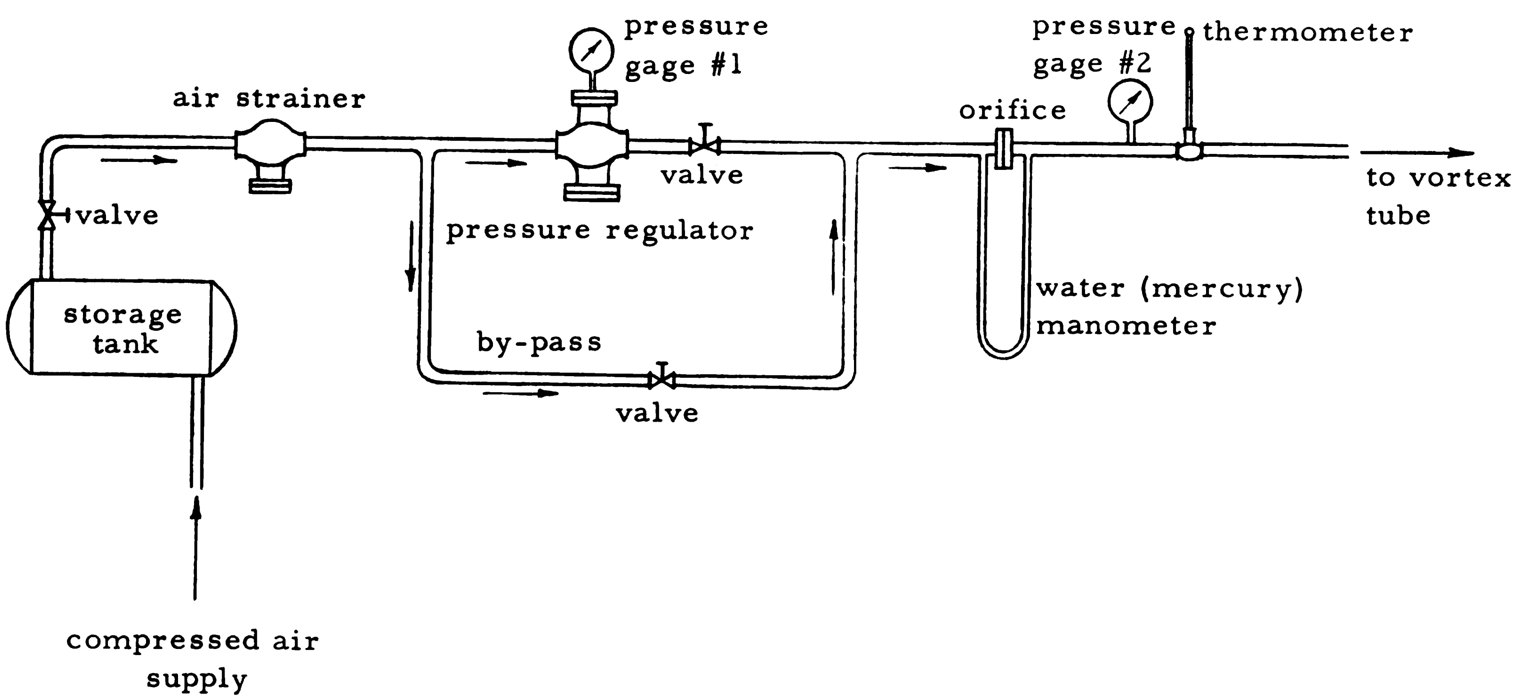

Figure 10. Flow diagram.

center block, and adjust the inlet valve opening to the vortex tube to the desired pressure. Second, the exit cone is turned all the way in, then backed out fairly slowly until the maximum Ranque-Hilsch (cooling) effect is obtained (in other words the lowest temperature attained inside the cold tube). This position of the vortex tube exit cone must be kept throughout the runs of the other center blocks with the same desired pressure adjusted by the inlet valve. After the reference is established the complete run can be accomplished in the following manner: (i) set up the uniflow tube with 90^{o} entry angle block and adjust the inlet valve opening to the vortex tube to the desired pressure; (ii) keep the exit cone at the reference position; (iii) after waiting until the steady condition is reached, obtain the traverse readings of static pressure, total pressure and total temperature by introducing the hypodermic probes for static pressure, total pressure, and total temperature, one at a time, into the vortex tube. Readings were taken every tenth of an inch by the probe which can be moved along the radial direction by means of the micrometer depth gage and slider assembly described in the section on apparatus. The traverses of static pressure, total pressure and total temperature were performed at each of the six stations (spaced 6.5 inches apart), with the inlet pressure maintained at a constant value throughout the whole run; (iv) replace the center block with others of various angles, one at a time, and repeat the procedure from (i) to (iii) until every entry angle of both the counterflow and uniflow tube has been tested.

As pointed out previously in the procedure, for every station, readings were recorded at every tenth of an inch, along the radius. For each radial position of a probe, two readings were taken, one corresponding to the probe above the tube center and the other corresponding to the probe below the center. The average of two readings is taken to be the value for the probe at the given radial position.

Test results: The measured quantities are the static pressures, total pressures, and total temperatures. The computed quantities are the velocities and static temperatures. The curves are plotted as total pressure, static pressure, total temperature, static temperature and velocity versus the radial distance from the center. Figures 11 to 16 show the velocity, pressure and temperature traverses for the uniflow tube corresponding to entry angles of 90° and 30° respectively. The traverses are for stations 2, 3 and 4 located in the mid-tube region so that end effects are minimized. It can be seen that the velocity has the characteristic of a "forced" vortex or wheel flow lasting for approximately eight diameters along the tube length, and that thereafter it is fairly uniform over the cross-section of the tube. The pressure and temperature curves display the same general characteristic for the two angles, but the curves for the 30° entry angle are flatter.

Figures 17 and 19 give the vortex strength and the maximum temperature separation for the uniflow tube corresponding to entry angles of 90° and 30°. It can be seen that the circulation and the temperature separation decrease with a decrease in entry angle. The decrease, however, is more pronounced when the entry angle is less than 45°. Above 45°, the vortex effect remains. Figures 18 and 20 show the variation of vortex strength and temperature separation in relation to the length. It can be seen that beyond station 4 or slightly more than nine diameters from the entrance, the vortex effect levels off, and any further lengthening of the tube is unnecessary.

The above applies to the uniflow vortex tube. For the case of the counterflow tube, Figures 21 to 26, give the velocity, pressure and temperature traverses, while Figures 27 to 30 give the vortex strength and temperature separation in relation to entry angle and tube length. The data show the same general characteristics as those for the uniflow tube. However, the counterflow tube gives larger temperature separation than the uniflow tube. This is because in the former, the cold and hot streams are allowed to separate immediately rather than allowed to mix along the entire length of the tube.

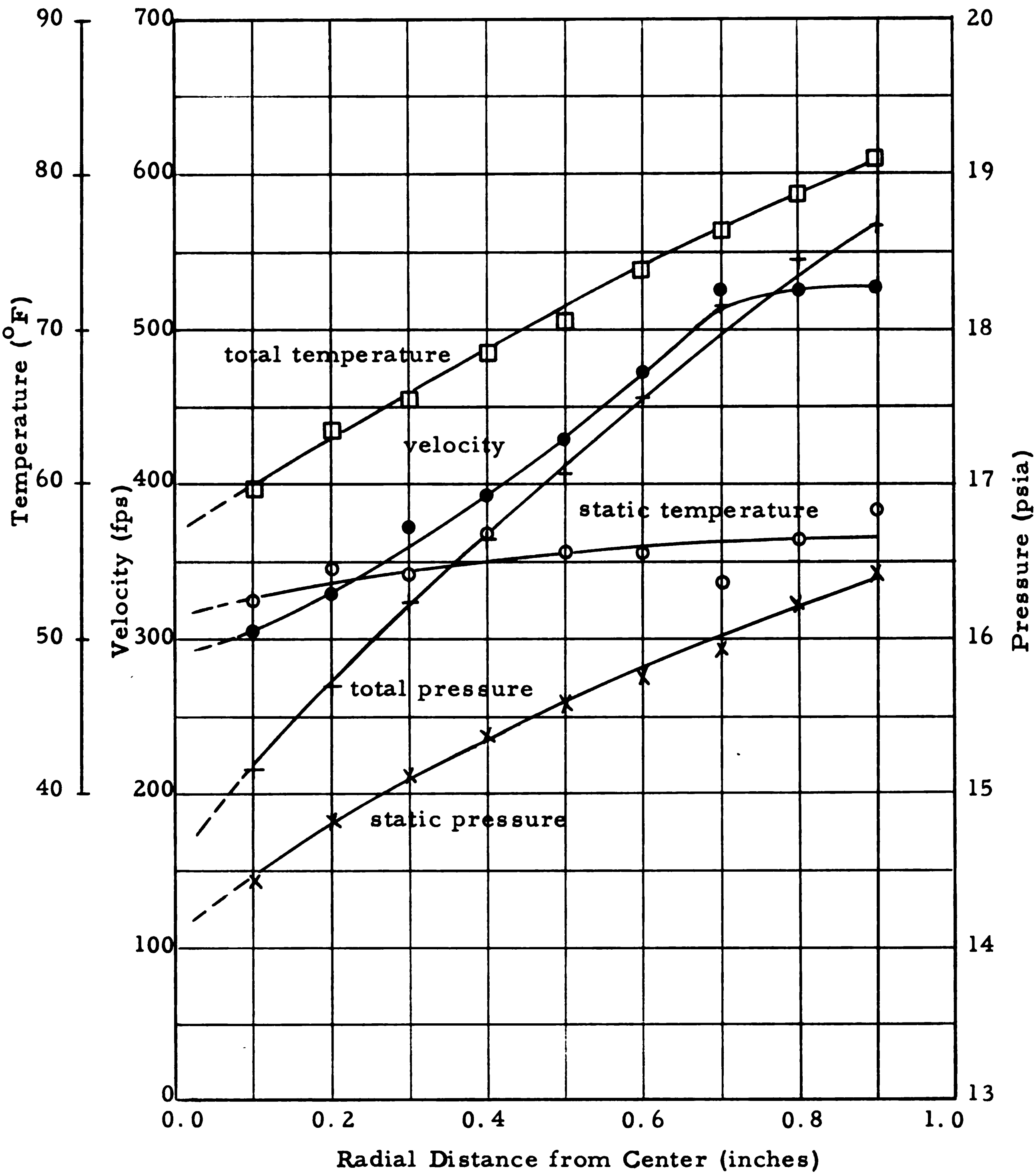

Figure 11. Velocity, pressure, and temperature traverse. Station 2. Entrance angle: 90°. Inlet pressure: 30 psig. Uniflow tube.

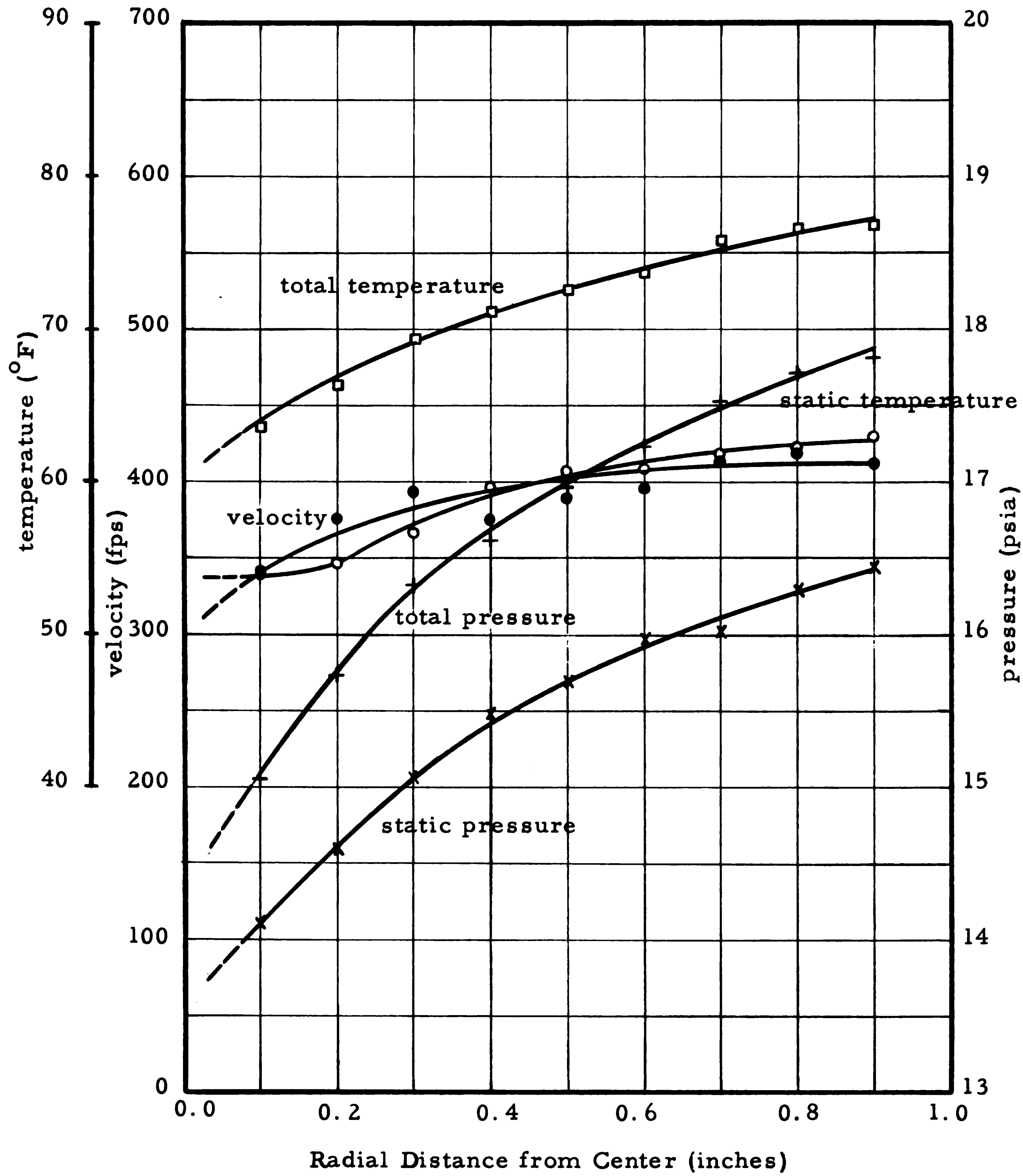

Figure 12. Velocity, pressure, and temperature traverse. Station 3. Entrance angle: 90°. Inlet pressure: 30 psig. Uniflow tube.

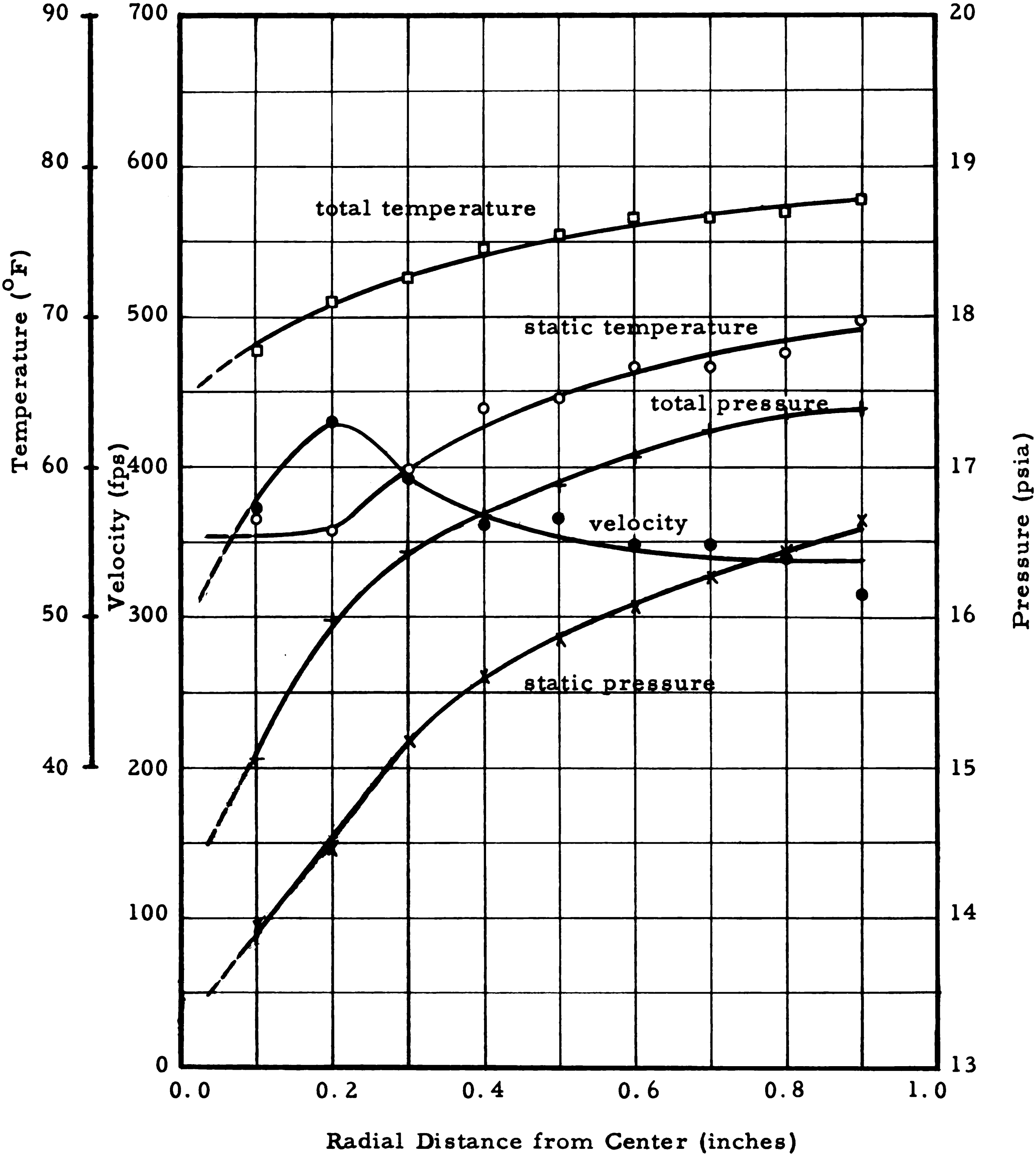

Figure 13. Velocity, pressure, and temperature traverse. Station 4. Entrance angle: 90°. Inlet pressure: 30 psig. Uniflow tube.

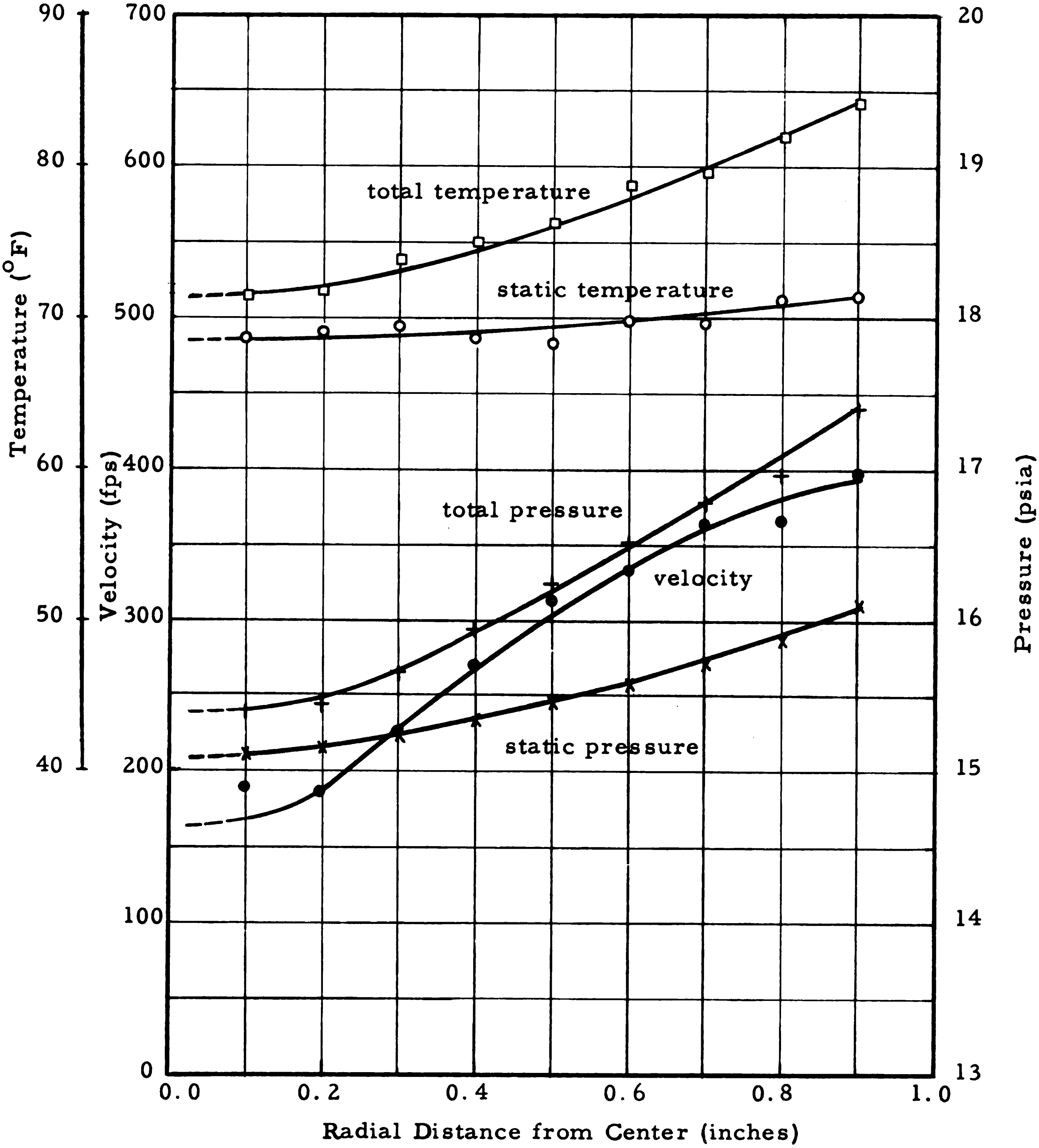

Figure 14. Velocity, pressure, and temperature traverse. Station 2. Entrance angle: 30°. Inlet pressure: 30 psig. Uniflow tube.

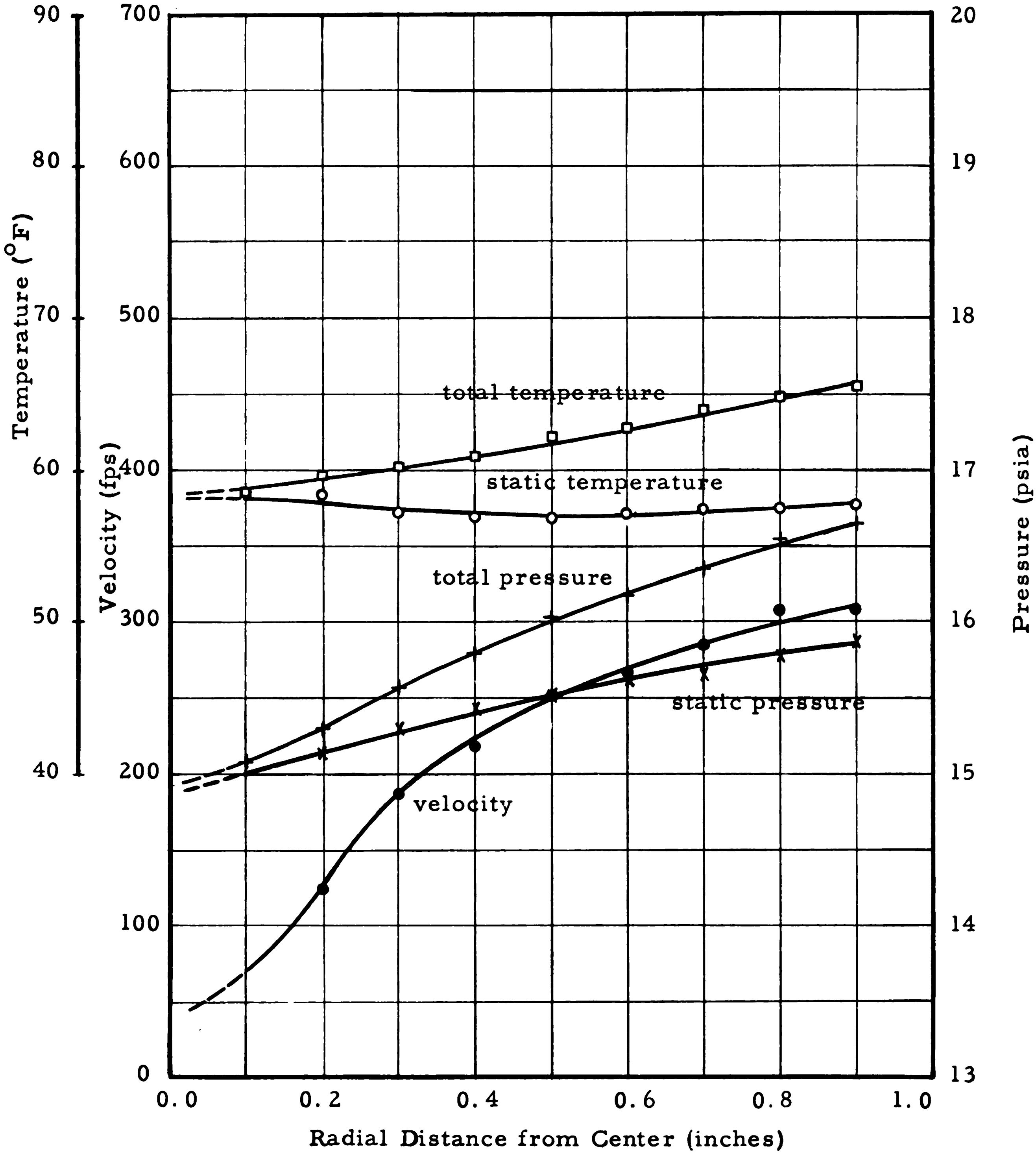

Figure 15. Velocity, pressure, and temperature traverse. Station 3. Entrance angle: 30°. Inlet pressure: 30 psig. Uniflow tube.

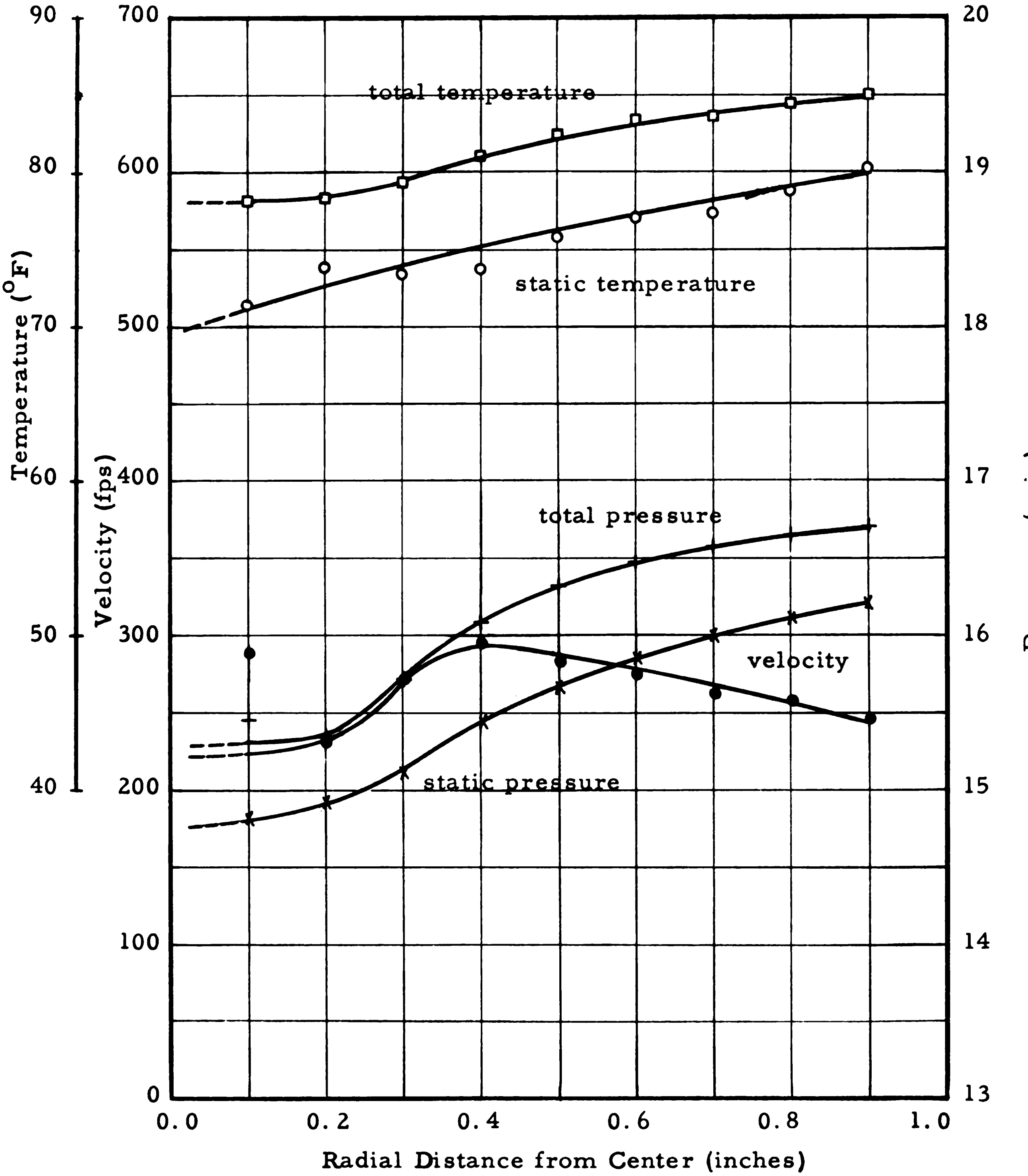

Figure 16. Velocity, pressure and temperature traverse. Station 4. Entrance angle: 30°. Inlet pressure: 30 psig. Uniflow tube.

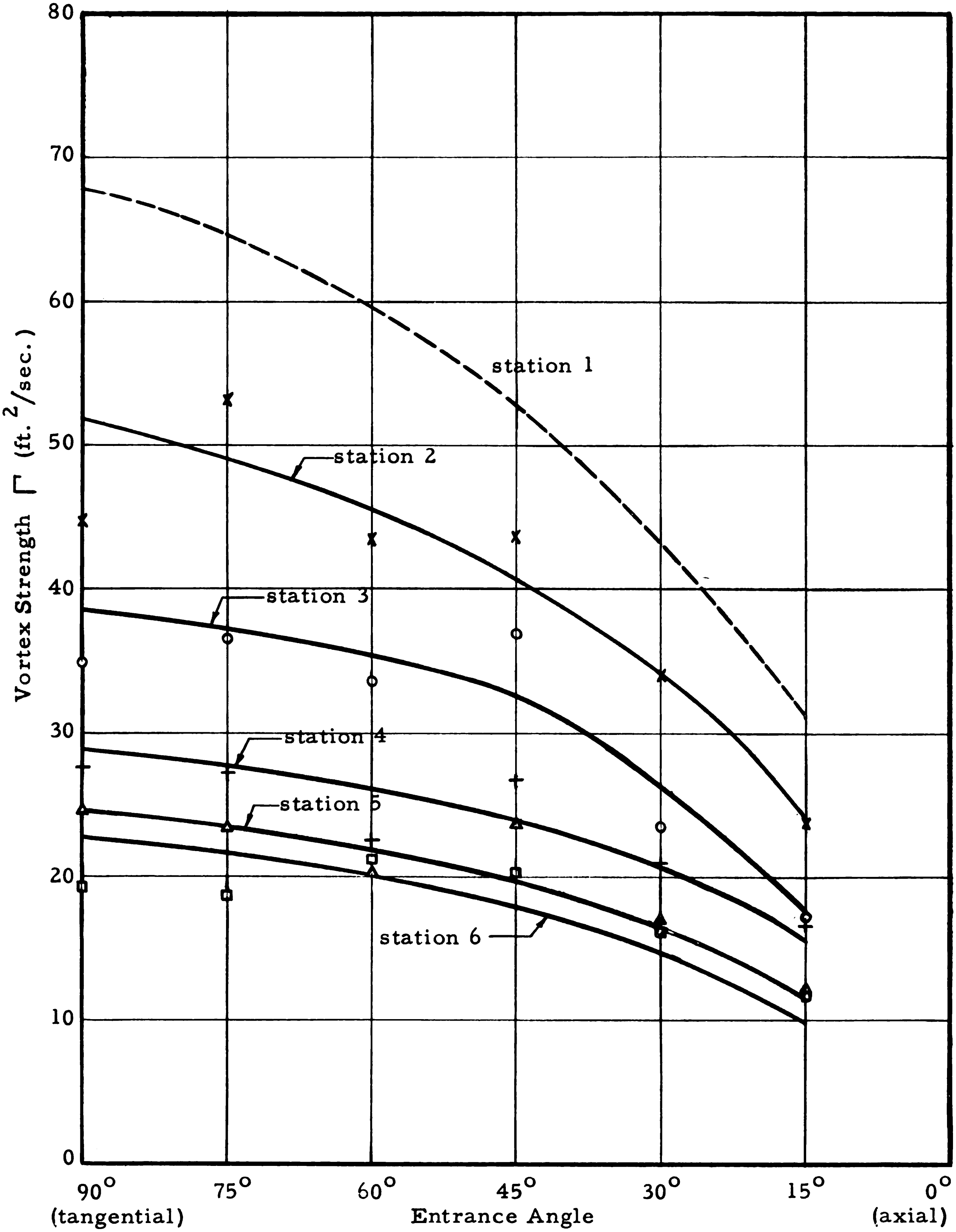

Figure 17. Vortex strength versus entrance angle. Inlet pressure: 30 psig. Uniflow tube.

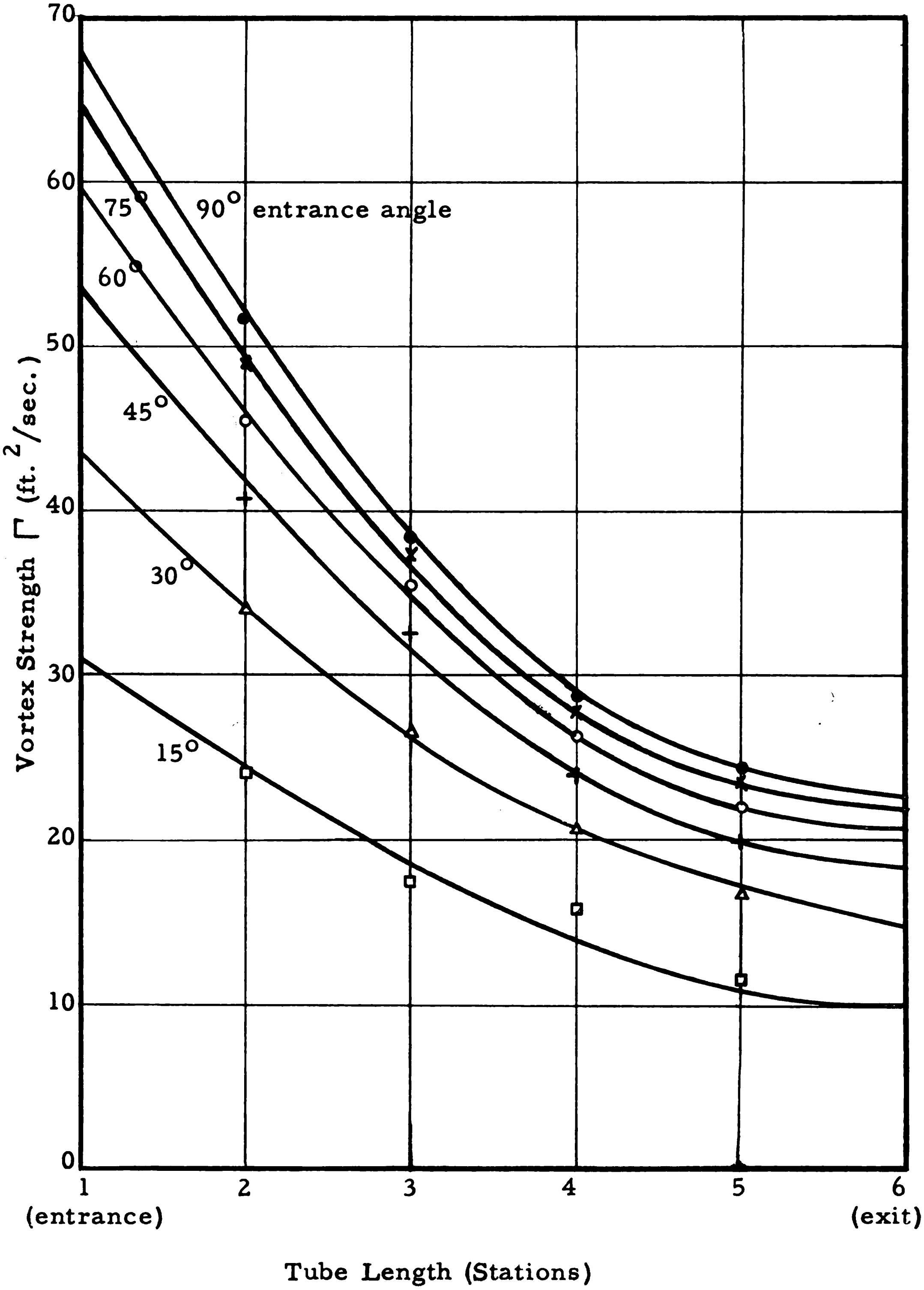

Figure 18. Vortex strength versus tube length.
Inlet pressure: 30 psig. Uniflow tube.

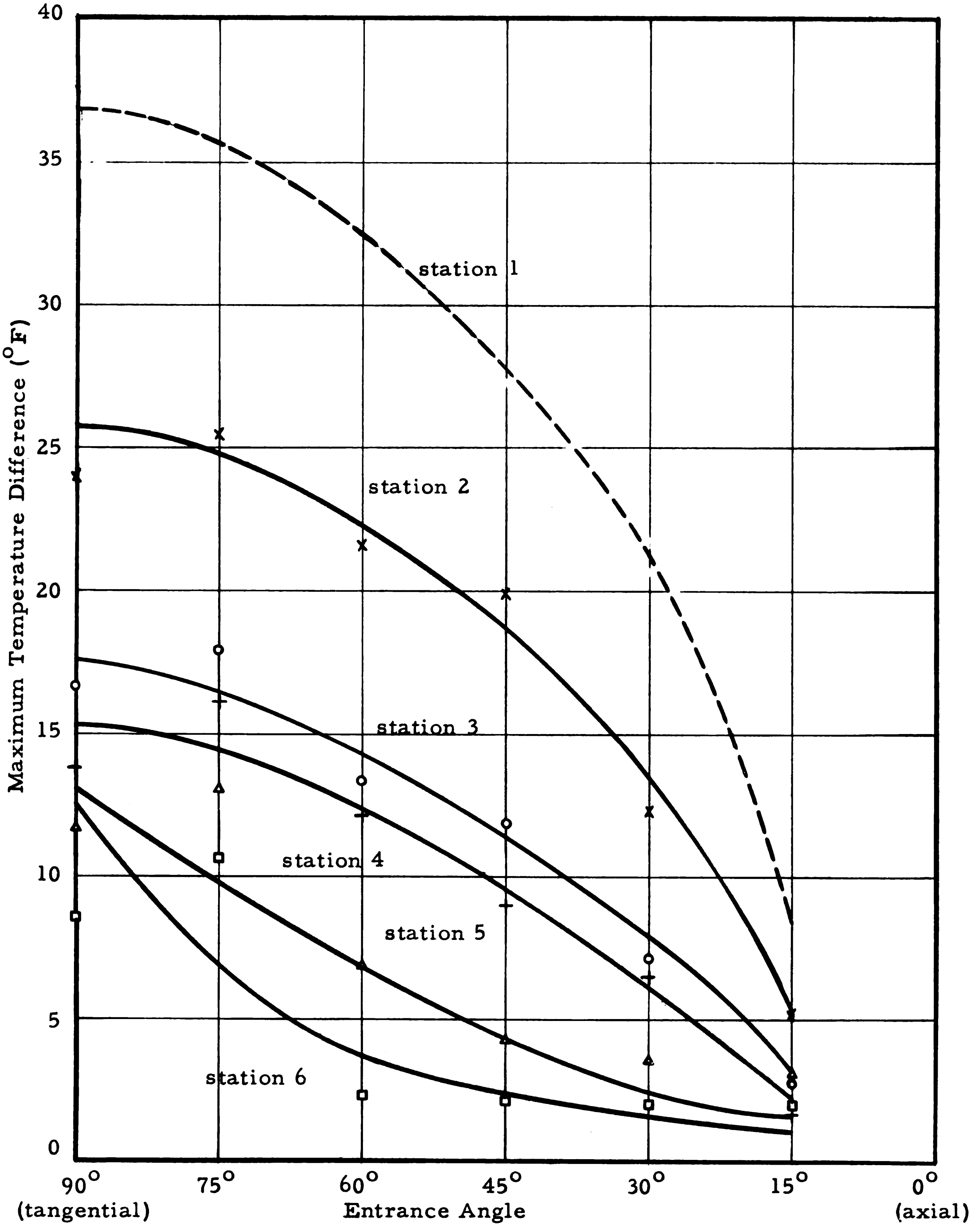

Figure 19. Temperature separation versus entrance angle.
Inlet pressure: 30 psig. Uniflow tube.

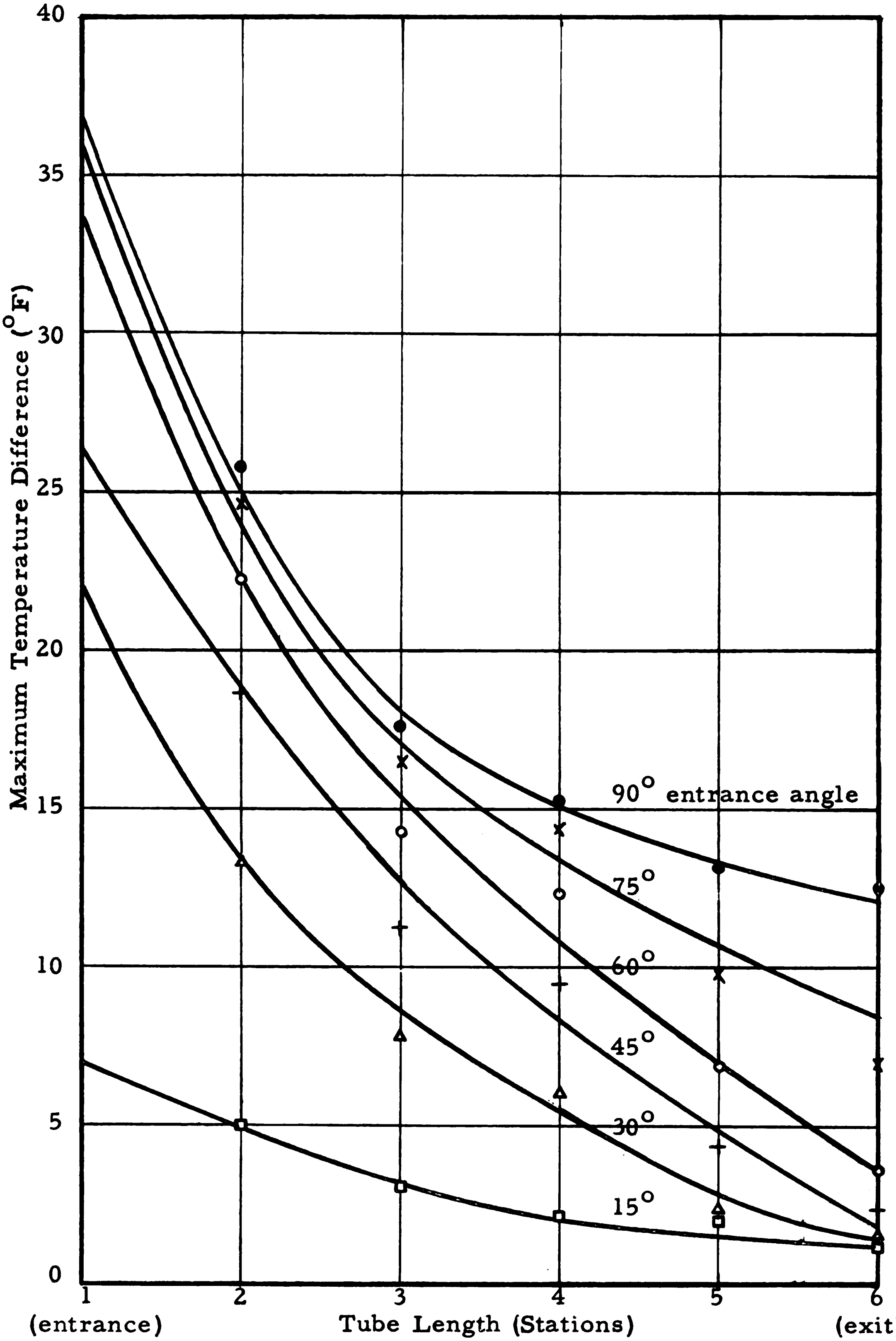

Figure 20. Temperature separation versus tube length. Inlet pressure: 30 psig. Uniflow tube.

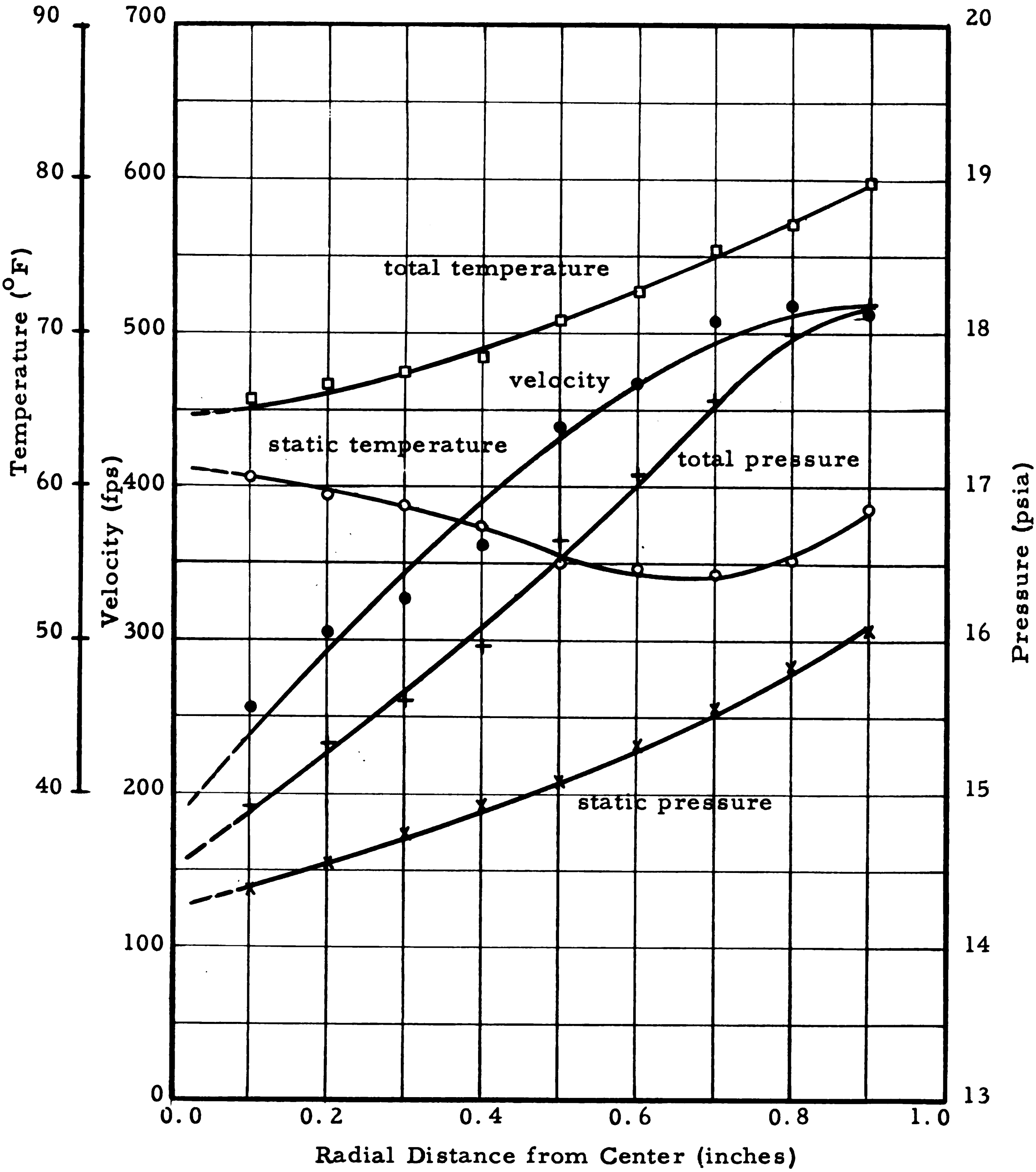

Figure 21. Velocity, pressure, and temperature traverse. Station 2. Entrance angle: 90°. Inlet pressure: 30 psig. Counter-flow tube.

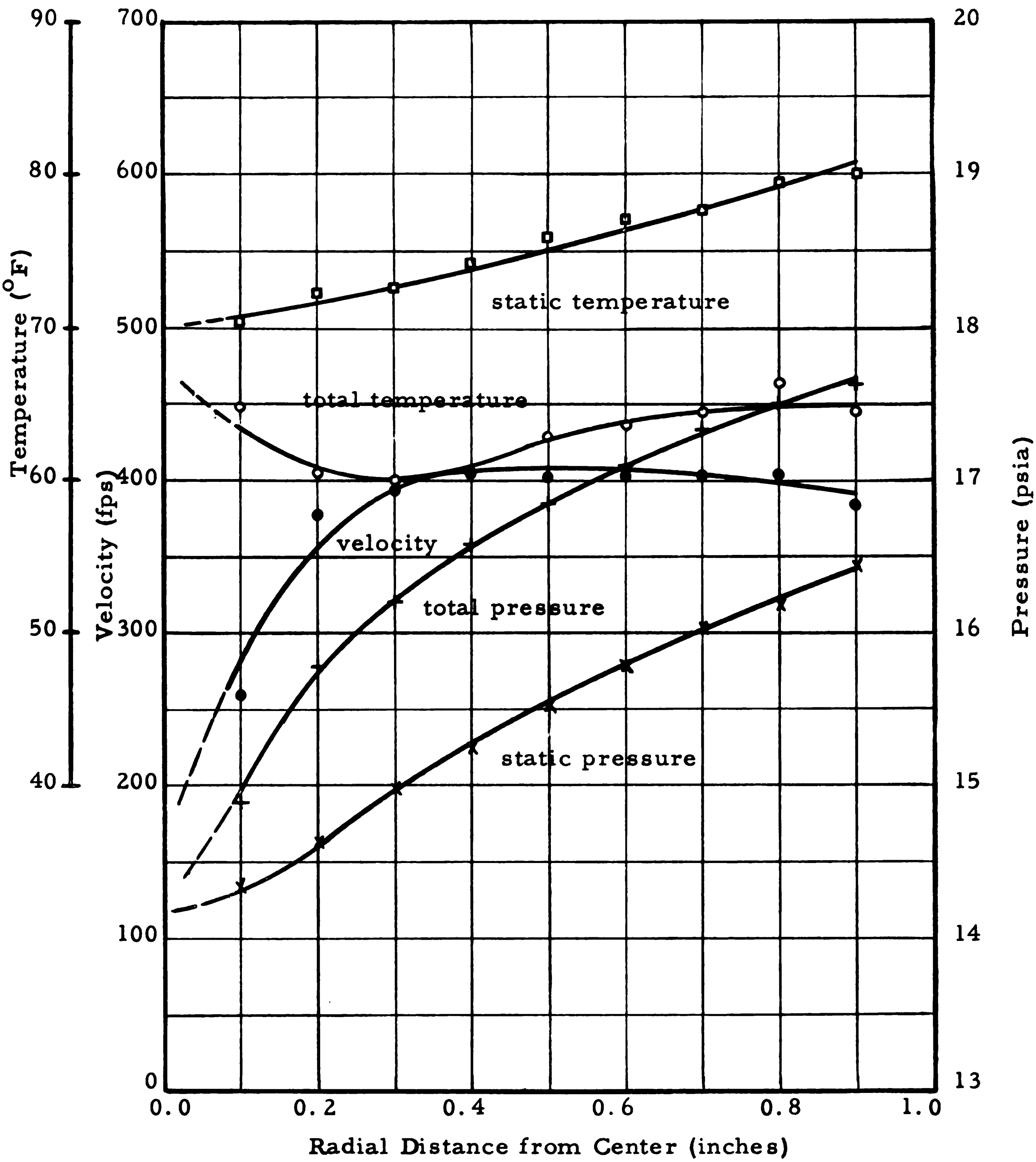

Figure 22. Velocity, pressure, and temperature traverse. Station 3. Entrance angle: 90°. Inlet pressure: 30 psig. Counter-flow tube.

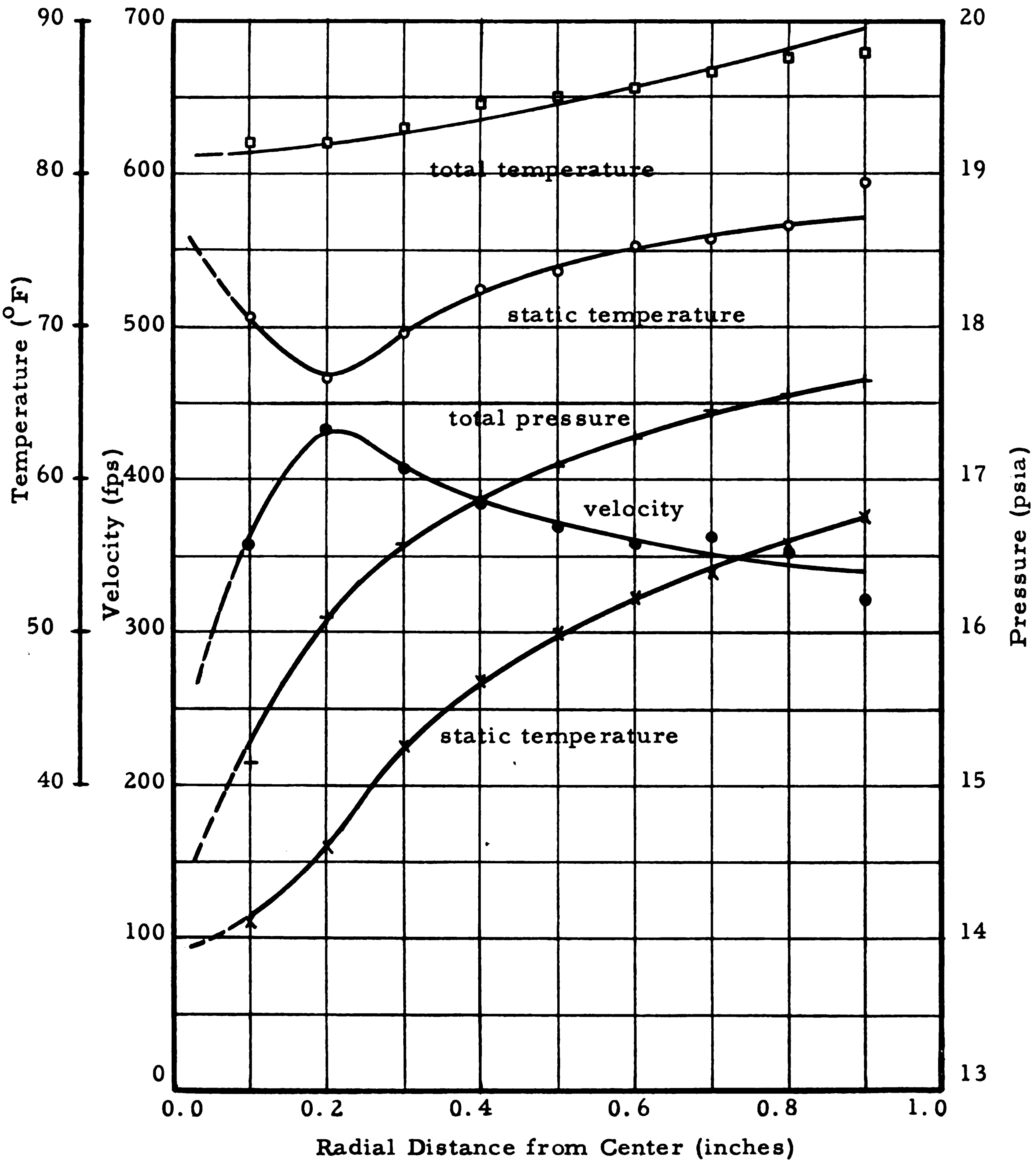

Figure 23. Velocity, pressure, and temperature traverse. Station 4. Entrance angle: 90°. Inlet pressure: 30 psig. Counter-flow tube.

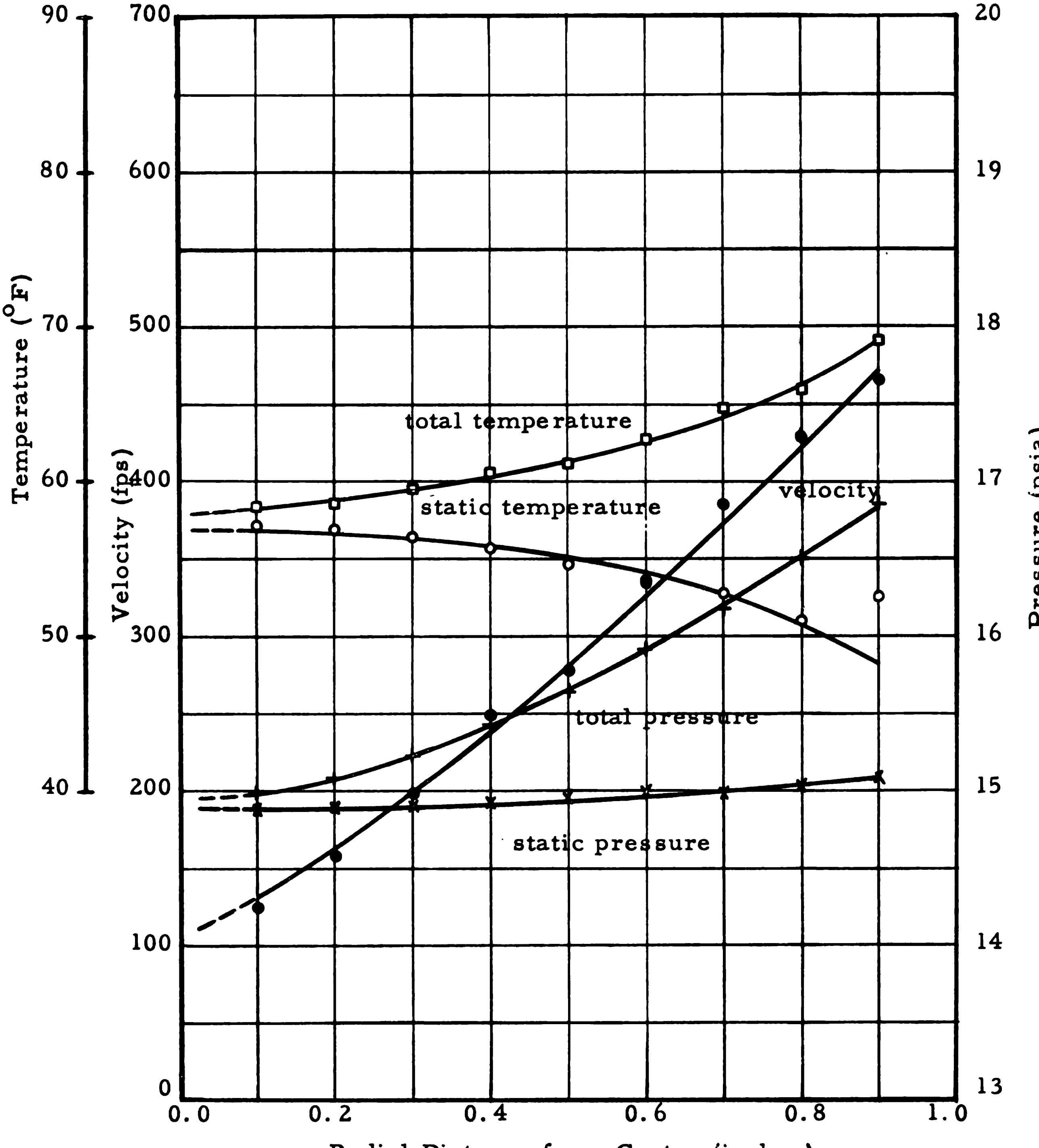

Figure 24. Velocity, pressure, and temperature traverse. Station 2. Entrance angle: 30°. Inlet pressure: 30 psig. Counter-flow tube.

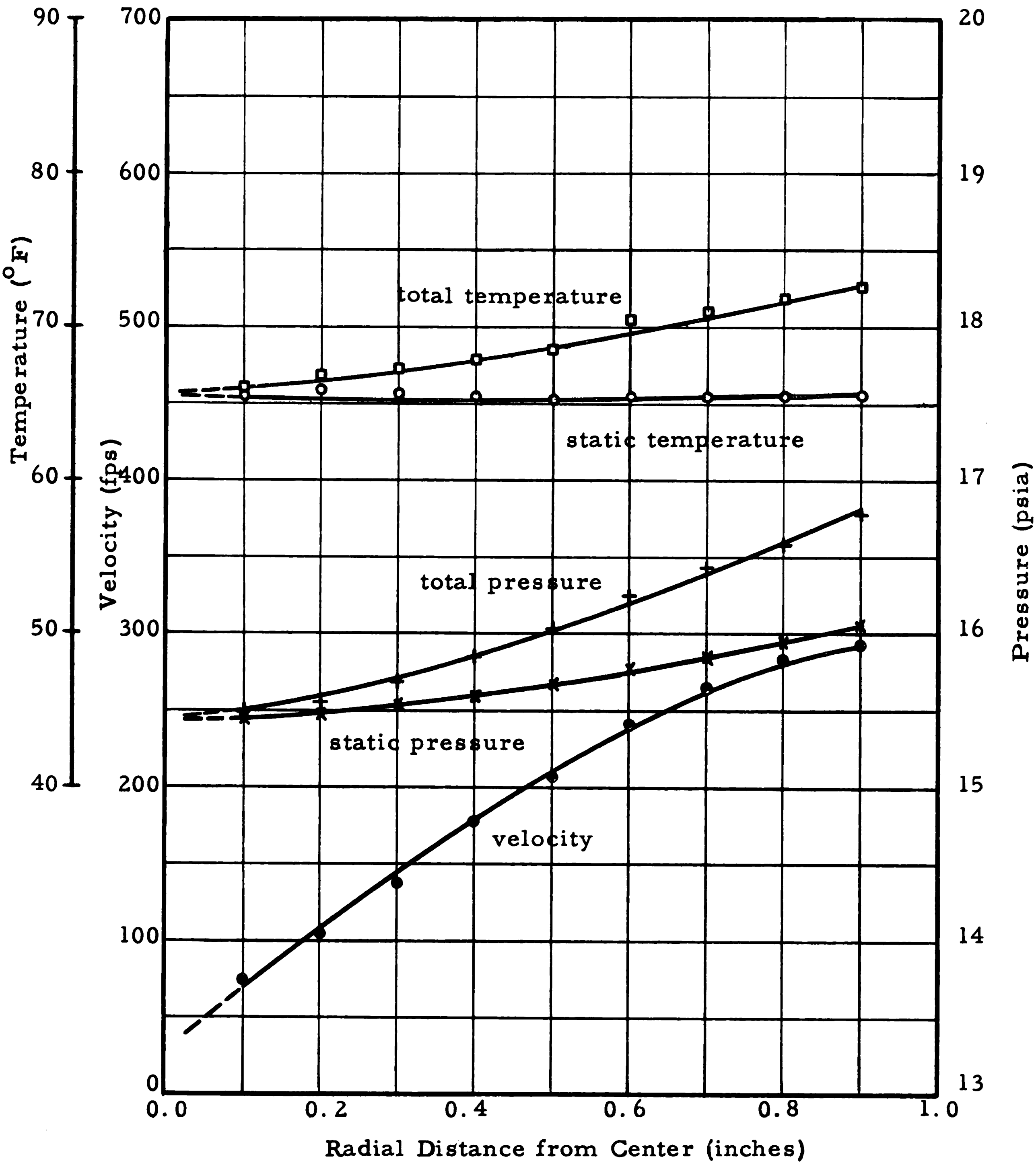

Figure 25. Velocity, pressure, and temperature traverse. Station 3. Entrance angle: 30°. Inlet pressure: 30 psig. Counter-flow tube.

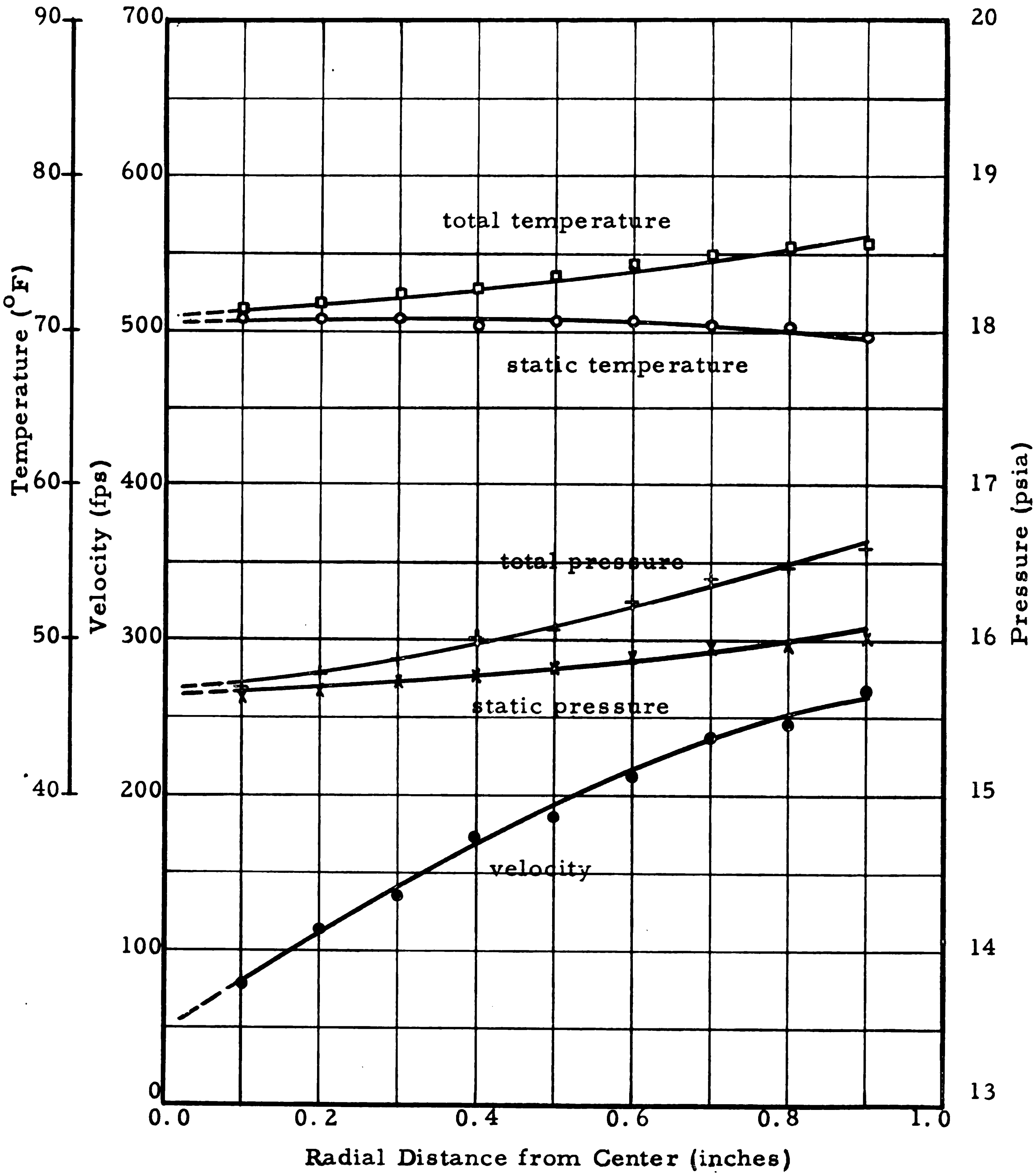

Figure 26. Velocity, pressure, and temperature traverse. Station 4. Entrance angle: 30°. Inlet pressure: 30 psig. Counter-flow tube.

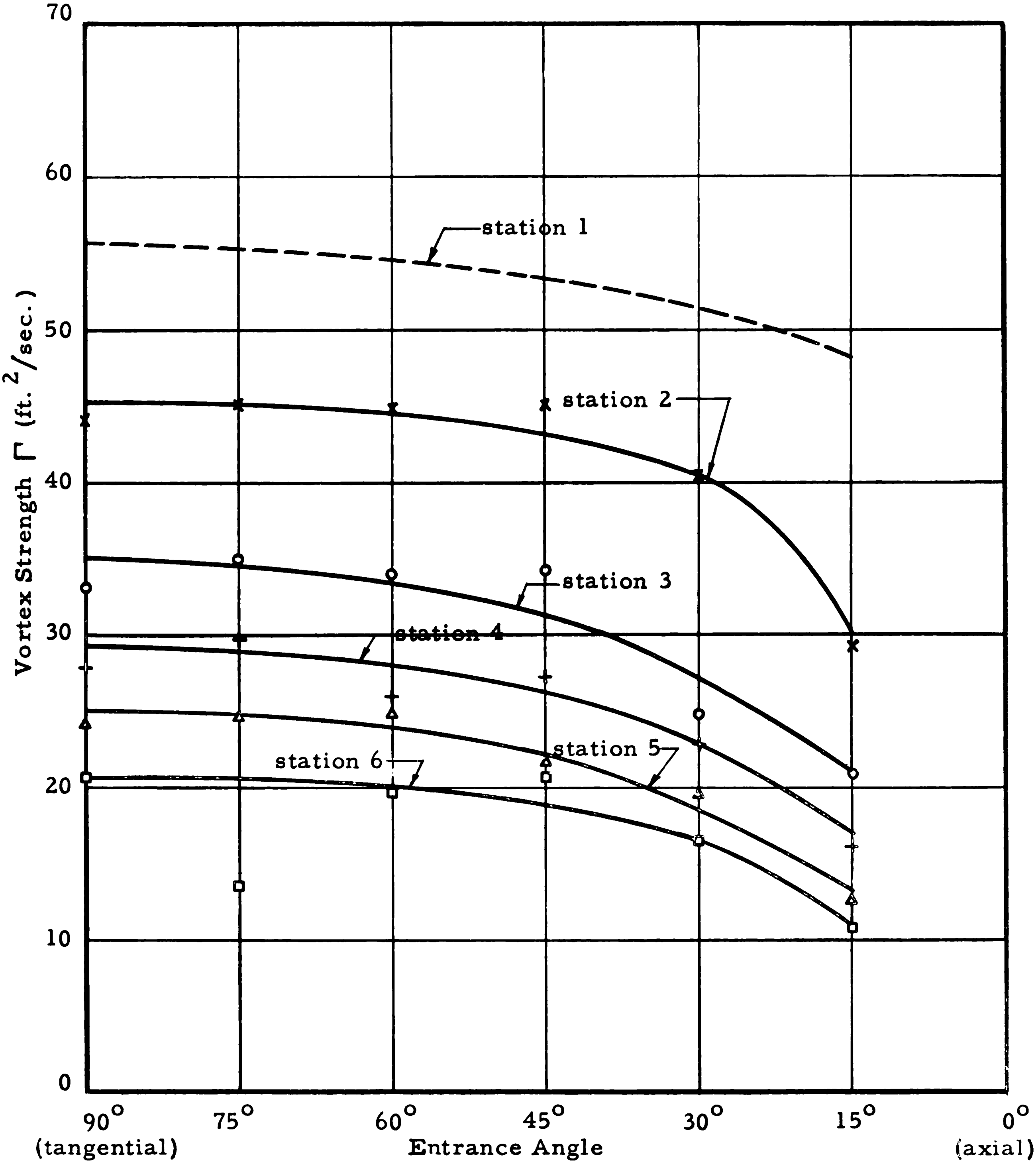

Figure 27. Vortex strength versus entrance angle.
Inlet pressure: 30 psig. Counter-flow tube.

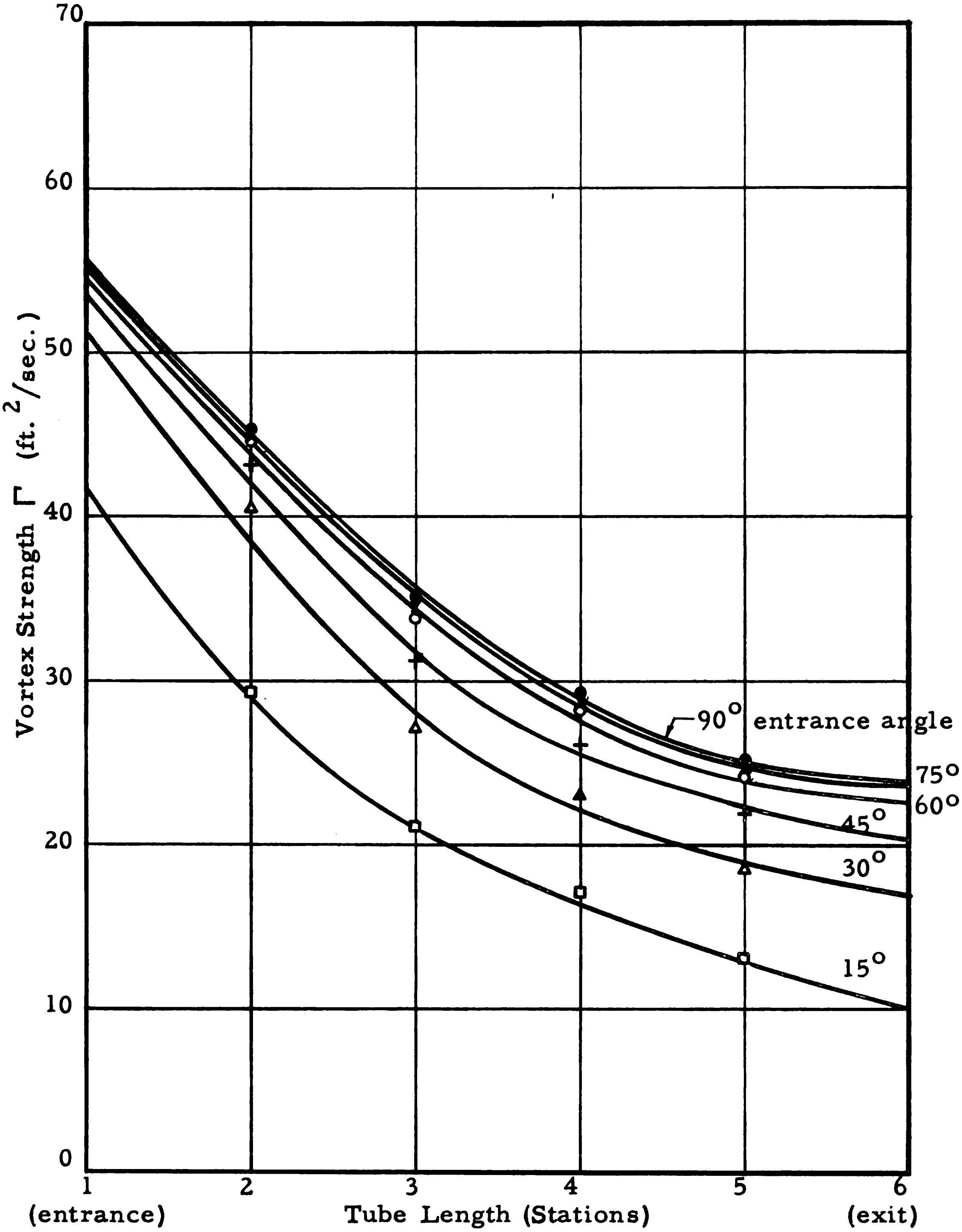

Figure 28. Vortex strength versus tube length.
Inlet pressure: 30 psig. Counter-flow tube.

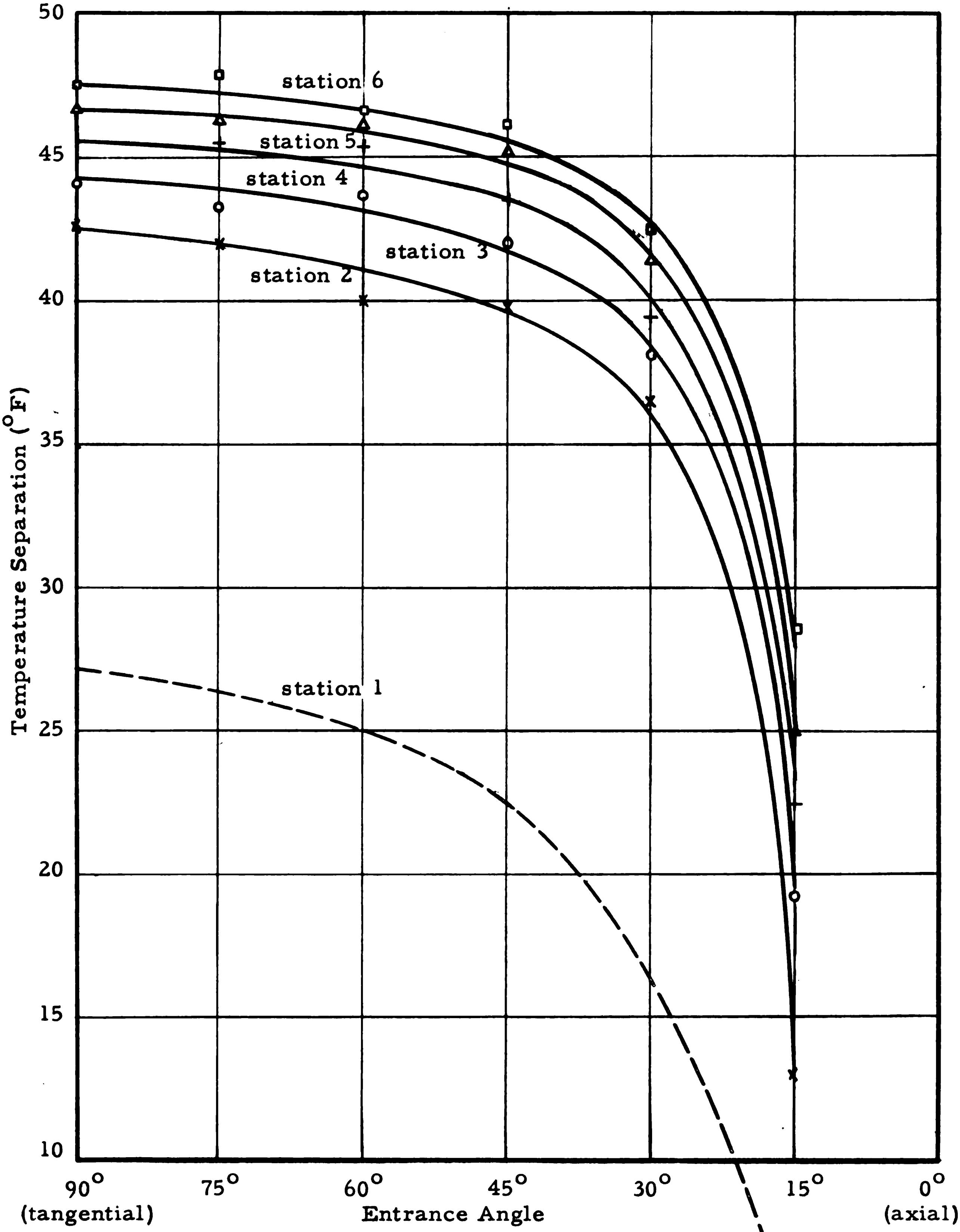

Figure 29. Temperature separation versus entrance angle. Inlet pressure: 30 psig. Counter-flow tube.

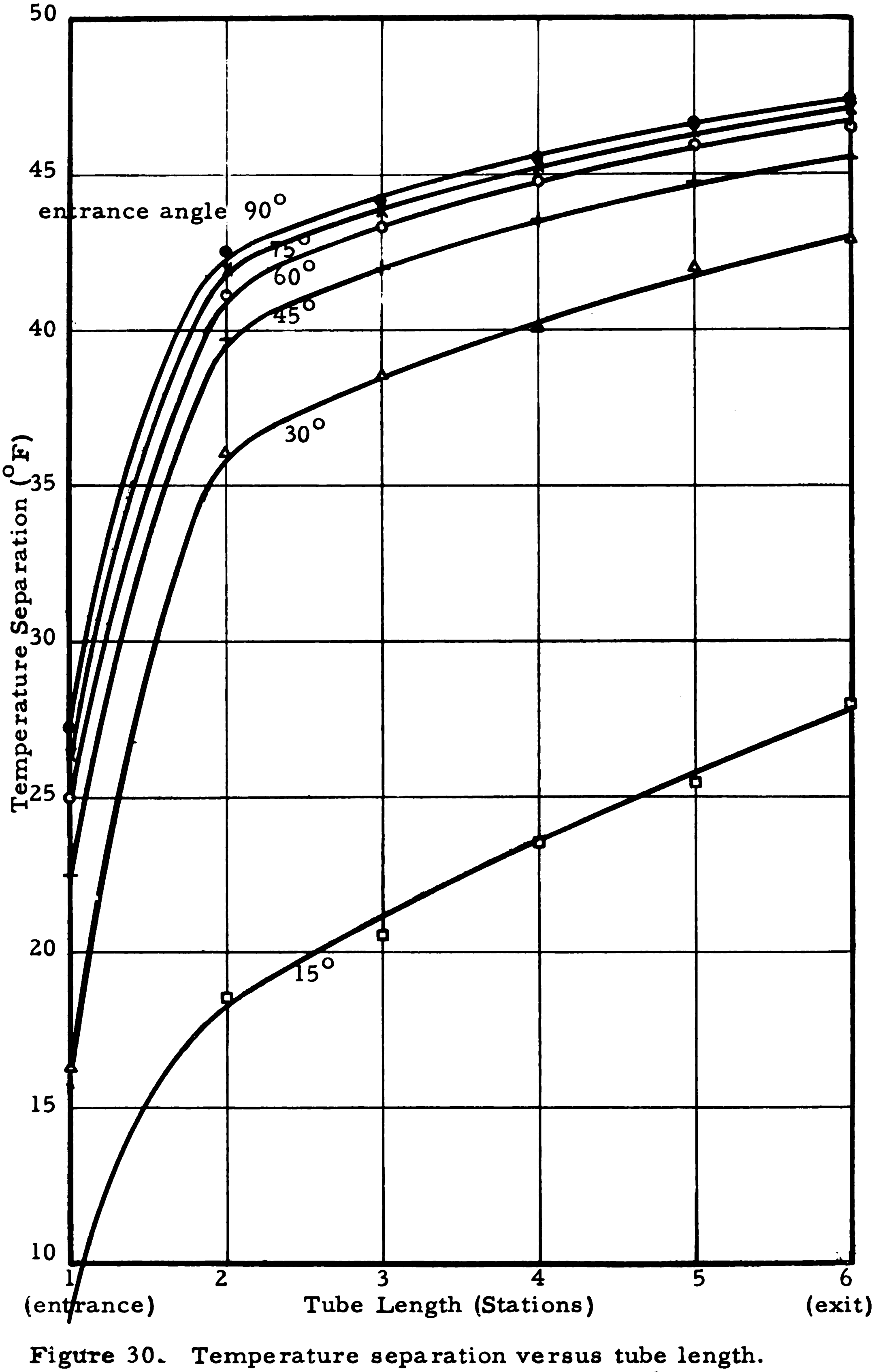

Figure 30. Temperature separation versus tube length. Inlet pressure: 30 psig. Counter-flow tube.

ANALYTICAL DEVELOPMENT

Basic equations of fluid flow: The theory of inviscid fluid flow, both incompressible and compressible, is based on the equations which follow:

Newton's equation: $$\rho \frac{d\vec{q}}{dt} = \rho \vec{F} - \text{grad } p \tag{1}$$

This is equivalent to the three scalar equations

$$\rho \frac{dq_x}{dt} = \rho F_x - \frac{\partial p}{\partial x}$$

$$\rho \frac{dq_y}{dt} = \rho F_y - \frac{\partial p}{\partial y}$$

$$\rho \frac{dq_z}{dt} = \rho F_z - \frac{\partial p}{\partial z}$$

With viscosity present, these equations will later be generalized by the inclusion of additional terms.

Equation of continuity: $$\text{div } (\rho \vec{q}) = -\frac{\partial \rho}{\partial t} \tag{2}$$

The above equations which express Newton's principle for the motion of an inviscid fluid and are usually referred to as Euler's equations, include one vector equation and one scalar equation, or four scalar equations. There are, however, five unknowns: q_x, q_y, q_z, ρ, and p, in these four equations. It follows that one more equation is needed in order that a solution of the system of equations be uniquely determined for given "boundary conditions." Boundary conditions, in a general sense, are equations involving the same variables, holding, however, not in the four-dimensional x, y, z, t-space, but only in certain sub-spaces as at some surface $\Phi(x, y, z) = 0$, for all t (boundary conditions in the narrower sense), or at some time $t = t_o$, for all x, y, z (initial conditions).

There exists no general physical principle which would supply a fifth equation to hold in all cases of motion of an inviscid fluid, as do equations (1) and (2). What can and must be added to (1) and (2) is some assumption that specifies the particular type of motion under consideration. This fifth equation will be called the specifying equation. Its general form is

$$F(p, \rho, \vec{q}, x, y, z, t) = 0 \tag{3}$$

Where it is understood that derivatives of p, ρ, and $\vec{q}$ may also enter **F**. The specifying equation used in this thesis is the equation of state $pv = RT$. Since the entropy of a perfect gas is given by

$$s = \frac{R}{\gamma - 1} \ln \frac{p}{\rho^{\gamma}} + \text{constant} \tag{4}$$

a curve for isentropic flow may be plotted as shown in Figure 31. Whenever the variation of p and ρ is confined to a small range of values, the relevant part of the curve can be approximated by a straight line to give a linearized form of p - ρ relation to facilitate the solution of the flow field.

p

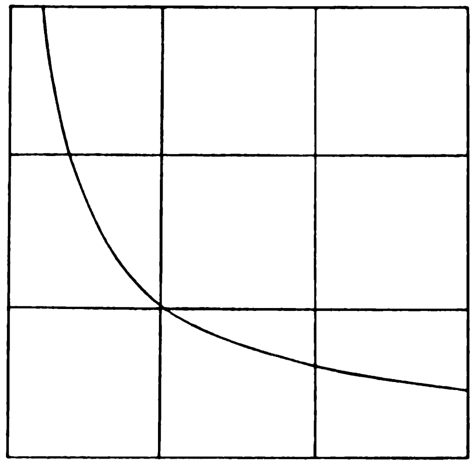

$\frac{1}{\rho}$

Figure 31. Isentropic Flow.

Energy equation: $$\frac{d}{dt}\left(\frac{q^2}{2} + gh + c_v T\right) + \frac{\operatorname{div}(p\vec{q})}{\rho} = Q \qquad (5)$$

This equation is a mathematical consequence of Newton's equation and the continuity equation. It does not depend upon the equation of state, but is arrived at by taking the scalar product on both sides of Newton's equation with $\vec{q}$ and transforming the scalar equation that results from this operation.

Influence of viscosity: For an inviscid fluid the forces exerted on any fluid element by surrounding masses are normal to the surface element on which they act and have the same intensity p, whatever the orientation of the surface element. The intensity p (force per unit area) is called the hydraulic pressure at the point under consideration. If viscosity is admitted, however, the stress vector on a surface element dS is no longer normal to dS. The stress can be resolved into a normal component σ and tangential or shearing component τ. The general form of Newton's equation, holding for any type of continuum, becomes

$$\rho \frac{d\vec{q}}{dt} = \rho\vec{F} - \text{grad } p + \vec{v} \qquad (6)$$

Where $\vec{v}$ is the resultant viscous force per unit volume. This equation, just as the energy equation for an inviscid fluid, can be obtained from the Newton's vector equation by scalar multiplication by $\vec{q}$. The result is

$$\frac{d}{dt}\left(\frac{q^2}{2} + gh + c_v T\right) + \frac{\text{div}\,(p\vec{q})}{\rho} + \frac{w'}{\rho} \qquad (7)$$

Where the additional term represents work done per unit mass and time against the viscous stresses at the surface of an element of fluid.

<u>Helmholtz and Kelvin Vortex Theory:</u>

<u>Circulation:</u> A kinematic motion useful in many problems of hydrodynamics is that of circulation, which may be defined as follows. Consider a simple closed curve $\mathfrak{C}$ in space together with a given sense of description (shown in Figure 32 by an arrow). On $\mathfrak{C}$, each element of arc can then be considered as an infinitesimal vector $d\vec{l}$, having the direction of the tangent to $\mathfrak{C}$. As usual, $\vec{q}$ denotes the instantaneous velocity at each point. If the scalar product of $\vec{q}$ and $d\vec{l}$ is integrated around the closed curve $\mathfrak{C}$, the line integral

$$\Gamma = \oint_{\mathfrak{C}} \vec{q} \cdot d\vec{l} = \oint_{\mathfrak{C}} q\cos(\vec{q}, d\vec{l})\, dl = \oint_{\mathfrak{C}} q_l\, dl \qquad (8)$$

is called the circulation around $\mathfrak{C}$.

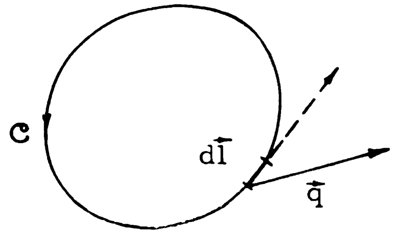

Figure 32. Circulation as Line Integral

The circulation is additive in the following sense. Suppose the closed curve $\mathbf{C}$ is "bridged" by some path AB (Figure 33). Give the two new closed curves ABDA and BAEB the same sense of description as $\mathbf{C}$. Then the circulations Γ_1 and Γ_2 respectively, along the new closed curves satisfy

$$\Gamma = \Gamma_1 + \Gamma_2 \tag{9}$$

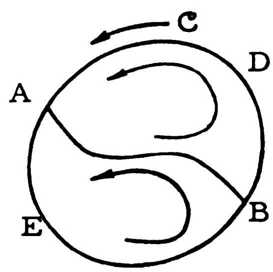

Figure 33. Illustration of Additivity of Circulation

In fact, the definition (8) shows that Γ_1 is the integral of $\vec{q} \cdot d\vec{l}$ along the path ABDA, which can be broken up into AB plus BDA. Similarly, Γ_2 is the integral along the path BA plus AEB. In the sum $\Gamma_1 + \Gamma_2$, the integrals along AB and BA cancel, since $\vec{q}$ is the same, while $d\vec{l}$ has opposite directions, along the two paths. Therefore the sum reduces to integrals along BDA and AEB, which is exactly the integral around $\mathfrak{C}$, i. e. Γ. The equation (9) can be generalized. Suppose $\mathcal{R}$ is any open two-sided surface spanning $\mathfrak{C}$, i. e., having $\mathfrak{C}$ as its rim. From one side of $\mathcal{R}$, the sense of description of $\mathfrak{C}$ appears counterclockwise, and normals to $\mathcal{R}$ will always be drawn out from this side. On $\mathcal{R}$ draw two sets of curves forming a network, as in Figure 34. Each mesh of the network is a closed curve, the sense of description being taken counterclockwise as viewed from the normal to the surface, and has a value of the circulation corresponding to it: Γ_1, Γ_2 . . . etc.

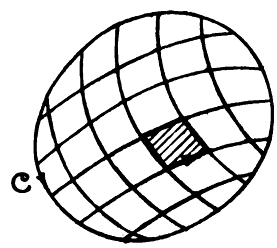

Figure 34. Circulation as Surface Integral

By repeated application of equation (9) it is seen that

$$\Gamma = \Gamma_1 + \Gamma_2 + . . . + \Gamma_n \tag{10}$$

Where n is number of meshes in the network. Now increase the number of "bridges" in such a way that the network becomes more dense and all meshes become smaller, while the number of terms in equation (10) increase. Let a function γ be defined at each point P of $\mathcal{R}$ as the limit of the quotient of the circulation along the contour of a mesh around P by the area of the mesh; meshes about that point becoming steadily smaller in all directions. For the first mesh, the circulation Γ_1 is then approximately given by $\gamma_1 \, d\mathcal{R}_1$ where $d\mathcal{R}_1$ is the area of the mesh and γ_1 the value of γ at some point in the mesh, the approximation becoming better as $d\mathcal{R}_1$ gets smaller; and similarly for the other meshes. Thus, as the number of terms increases indefinitely, the right-hand member of equation (10) yields the surface integral of γ over $\mathcal{R}$, or

$$\Gamma = \int_{\mathcal{R}} \gamma d\mathcal{R} \tag{11}$$

From the definition of γ, it is obvious that the value of this function at any point of $\mathcal{R}$ depends upon the distribution of the velocity $\vec{q}$ in neighborhood of this point. In computing this relationship choose curves on $\mathcal{R}$ which always cross at right angles. Then at any point P, set up a regular coordinate system, taking the z-axis in the direction of the normal to $\mathcal{R}$ at P and the x- and y-directions tangent to the two curves through P so as to form a right-handed coordinate system. An infinitesimal mesh starting at P is of the type illustrated in Figure 35.

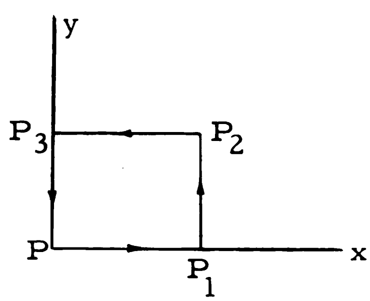

Figure 35. Circulation around Infinitesimal Mesh

In computing the line integral equation (8) for this mesh, the path may be broken up into four infinitesimal elements, and $q_l dl$ evaluated for each part. Along PP_1 the contribution is $q_x dx$, along P_1P_2 it is

$$[q_y + (\frac{\partial q_y}{\partial x}) dx] dy,$$

along P_2P_3 it is $-[q_x + (\frac{\partial q_x}{\partial y}) dy] dx$, and along P_3P it is $-q_y dy$. The sum of these terms gives the integral along the whole path, and the circulation along the contour of this infinitesimal mesh is therefore

$$d\Gamma = (\frac{\partial q_y}{\partial x} - \frac{\partial q_x}{\partial y}) dx dy \tag{12}$$

Since dxdy is the area of this mesh, the function γ must have the value

$$\frac{\partial q_y}{\partial x} - \frac{\partial q_x}{\partial y} \quad \text{at } P.$$

Now this quantity is exactly the z-component of the vector known as the curl of $\vec{q}$, defined by

$$\text{curl } \vec{q} = (\frac{\partial q_z}{\partial y} - \frac{\partial q_y}{\partial z}, \frac{\partial q_x}{\partial z} - \frac{\partial q_z}{\partial x}, \frac{\partial q_y}{\partial x} - \frac{\partial q_x}{\partial y}) \tag{13}$$

It is to be noted that this definition of curl $\vec{q}$ is valid in any rectangular right-handed coordinate system. Since the z-direction is that of the normal to the surface $\mathcal{R}$, it appears that γ has the value of the component of curl $\vec{q}$ normal to the surface

$$\gamma = (\text{curl } \vec{q})_n \tag{14}$$

Thus, equation (11) may be written as

$$\Gamma = \int_{\mathcal{R}} (\text{curl } \vec{q})_n \, d\mathcal{R} \tag{15}$$

and this formula is independent of the coordinate system used. If a vector $d\vec{\mathcal{R}}$ be introduced, having magnitude $d\mathcal{R}$ and the direction of the normal to the surface, equation (15) may also be written as

$$\Gamma = \int (\text{curl } \vec{q}) \cdot d\vec{\mathcal{R}} \tag{15'}$$

When the two equations (8) and (15') are combined, the result is

$$\oint \vec{q} \cdot d\vec{l} = \int (\text{curl } \vec{q}) \cdot d\vec{\mathcal{R}}$$

This vector formula is known as Stokes' theorem. When $\vec{q}$ is the velocity of flow, it states that the circulation along any closed curve is given by the surface integral of curl $\vec{q}$ over any surface spanning the closed curve.

It is obvious that equations (15) and (15') can be applied only if it is possible to find some surface that has the given closed curve as rim and on which curl $\vec{q}$ is defined everywhere. For example, in the case of a flow around an infinite cylindrical obstacle, no such surface can be found for any closed curve which surrounds the cylinder. Even here the theorem can be applied to give a somewhat different result. As shown in Figure 36, two such closed curves $\mathcal{C}_1$ and $\mathcal{C}_2$, can, by a bridge AB, be combined in a single closed curve for which a suitable spanning surface exists. Then the integral equation (15) extended over this surface gives $\Gamma_1 - \Gamma_2$, since $\mathcal{C}_2$ is given a reverse orientation and the contribution from AB cancel. In particular, if curl $\vec{q} \equiv 0$ in the domain of flow (irrotational flow), then $\Gamma_1 - \Gamma_2 = 0$ or $\Gamma_1 = \Gamma_2$: the circulation is equal for all closed curves surrounding the obstacle.

Mean rotation: The vector curl $\vec{q}$ defined by equation (13) can be given a simple kinematic interpretation. Let P be a point of the moving mass, and let Q be a neighboring point. In rigid-body rotation with angular velocity ω about an axis through P, the curl of the velocity at Q is the same, namely 2ω, no matter where Q is situated. This is not so in the case of a fluid or of any deformable mass.

Start by computing the angular velocity of PQ about an arbitrary given axis through P: Taking P as the origin, choose a right-handed rectangular coordinate system such that the z-direction is that of the axis. Let PQ = dr and Q' be the projection of Q onto the x, y-plane (Figure 37), θ the angle between the z-axis and PQ and ϕ the angle between the x-axis and PQ'. Then the distance from the z-axis to Q is PQ' = $\sin\theta dr$, and the rectangular coordinates of Q, relative to P, are given by $dx = \cos\phi \sin\theta dr$, $dy = \sin\phi \sin\theta dr$, and $dz = \cos\theta dr$.

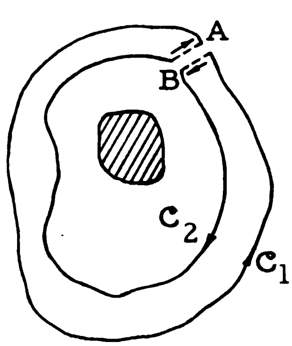

Figure 36. Closed Curve Surrounding Obstacle

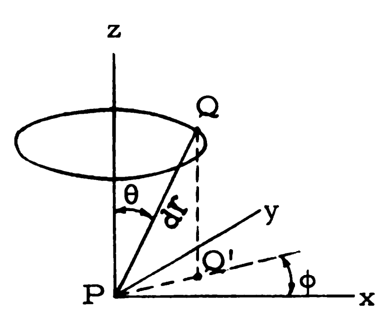

Figure 37. Computation of Mean Rotation

Therefore, if the velocity at P is $\vec{q}$, the velocity vector at Q (relative to P) is

$$\left[\frac{\partial \vec{q}}{\partial x} \cos\phi \sin\theta + \frac{\partial \vec{q}}{\partial y} \sin\phi \sin\theta + \frac{\partial \vec{q}}{\partial z} \cos\theta\right] dr.$$

The angular velocity of the segment PQ about the z-axis is obtained by dividing the distance from the z-axis to Q, i. e. PQ', into the component of the velocity at Q in the direction which is perpendicular to PQ' and to the z-axis. The angles which this direction makes with the x-, y- and z-axes are $\phi+90^{\circ}$, ϕ, and 90°, respectively, and the consines of these angles are $-\sin\phi$, $\cos\phi$, and 0. Thus the required component is

$$\left[\frac{\partial q_y}{\partial x} \cos^2\phi - \frac{\partial q_x}{\partial y} \sin^2\phi - \left(\frac{\partial q_x}{\partial x} - \frac{\partial q_y}{\partial y}\right) \sin\phi \cos\phi\right] \sin\theta dr$$
$$+ \left[\frac{\partial q_y}{\partial z} \cos\phi - \frac{\partial q_x}{\partial z} \sin\phi\right] \cos\theta dr$$

Division by $\sin\theta dr$ then gives the angular velocity of PQ about the z-axis, the value depending, in general, on the coordinates θ and ϕ of Q.

Now, compute the average angular velocity for all points, Q on the same circle of latitude θ = constant, on the sphere dr = constant, by first integrating with respect to ϕ from 0 to 2π and then dividing by 2π. All integrals vanish except those of the first two terms, giving

$$\frac{1}{2\pi}\left[\frac{\partial q_y}{\partial x}\int_0^{2\pi} \cos^2\phi d\phi - \frac{\partial q_x}{\partial y}\int_0^{2\pi} \sin^2\phi d\phi\right] = \frac{1}{2}\left(\frac{\partial q_y}{\partial x} - \frac{\partial q_x}{\partial y}\right) = \frac{1}{2}(\text{curl}\,\vec{q})_z \qquad (16)$$

This result being independent of θ and dr, the same value is obtained for the average or mean angular velocity about the z-axis of the whole infinitesimal sphere at P. Also, the z-direction could be any direction, so the above result shows that at any point P of the moving fluid, the vector $\frac{1}{2}$ curl $\vec{q}$ represents the (instantaneous) mean angular velocity or mean rotation for all segments PQ within an infinitesimal sphere of center P. It may be called as the mean rotation or mean angular velocity of the fluid element around P. Excluding the case curl $\vec{q} \equiv 0$, equation (13) defines at each moment t at each point of the fluid a vector curl $\vec{q}$ which is twice the mean angular velocity of the fluid element around P. This vector is usually called the vortex vector. Any line within the fluid which at each of its points has the same direction as curl $\vec{q}$ is called a vortex line. All vortex lines passing through the points of a closed curve $\mathfrak{C}$, not itself a vortex line, form a vortex tube. The lateral surface of the tube is called its mantle. A vortex tube of infinitesimal cross section is called a vortex.

For any closed curve, such as $\mathfrak{C}$, in Figure 38, which lies on the mantle of a vortex tube but not encircling the tube, the circulation must be zero. This follows from equation (15). Since a surface $\mathcal{R}$ spanning this closed curve can be taken on the mantle, where the normal component of curl $\vec{q}$ is everywhere zero. This is no longer true for a close curve which encircles the tube, as C or C_2 in Figure 38. Here it follows from equation (15) that the circulation must have a common

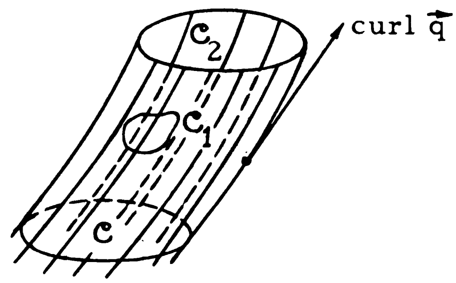

Figure 38. Vortex Tube with Various Closed Curves

value for all closed curves encircling the same tube. In fact, in computing the circulation Γ_2 along $\mathfrak{C}_2$ one can choose for $\mathcal{R}_2$ the surface consisting of the part of the mantle between $\mathfrak{C}_2$ and $\mathfrak{C}$ together with any surface $\mathcal{R}$ spanning $\mathfrak{C}$. As above, the surface integral is zero on the mantle, so that the integral over $\mathcal{R}_2$ has exactly the same values as the integral over $\mathcal{R}$, giving $\Gamma_2 = \Gamma$. This common value of the circulation is also called the vorticity of the tube; it is a scalar quantity, not to be confused with the magnitude of the vortex vector. In the case of a vortex filament, the vorticity $d\Gamma$ is given by the product of the length of the vortex vector by the normal cross section of the tube.

If a vortex tube be divided into several tubes of finite cross section (or into an infinite number of vortex filaments), the vorticity of the whole tube is the sum (integral) of the individual vorticities. This follows from the additivity of circulation [or from equation (15)].

A vortex tube cannot begin or end in the interior of the fluid, but must either be a closed tube (like a torus or doughnut) or else (provided it does not meet a boundary) must extend indefinitely in either direction. For at an end, if there were one, a continuous transition would be possible along the mantle from curves of type $\mathfrak{C}_1$ to those of type $\mathfrak{C}_2$, which is inconsistent with the fact that $\Gamma_1 = 0$ while $\Gamma_2 = \text{constant} \neq 0$

<u>Kelvin's Theorem</u>: The concepts of circulation and mean rotation, as well as the relation between them, are valid for any type of continuously distributed material. Consider the case of an inviscid elastic fluid. The fluid particles lying on any closed curve at same moment will still form a closed curve at a later time, for reasons of continuity no separation of particles can occur; a preliminary question, and one which can be given a very simple and decisive answer, is the following: How does the circulation change during this transition?

In Figure 39, the solid line represents a closed curve $\mathfrak{C}$, and the dotted line the closed curve $\mathfrak{C}'$ formed by the same material particles after time dt. The circulations along these two closed curves are given by

$$\Gamma = \oint \vec{q} \cdot d\vec{l} \text{ and } \Gamma' = \oint \vec{q}' \cdot d\vec{l}' \qquad (17)$$

where the integrals are evaluated along $\mathfrak{C}$ and $\mathfrak{C}'$ respectively. Let P be the position of an arbitrary particle of $\mathfrak{C}$ and Q that of a particle of $\mathfrak{C}$ at a distance dl away, and let P' and Q' be the positions of these particles after time dt. Then

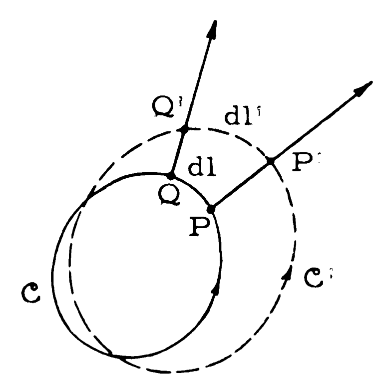

Figure 39. Two Closed Curves for Same Particles

$$\overline{PP'} = \vec{q}dt \text{ and } \overline{QQ'} = (\vec{q} + \frac{\partial \vec{q}}{\partial l} dl) dt$$

Where $\partial/\partial l$ denotes the directional derivative in the direction of the tangent to C at P. The corresponding element of arc $d\vec{l}'$ on C' can be computed from the vector equation, $\overline{PP'} + \overline{P'Q'} = \overline{PQ} + \overline{QQ'}$, giving

$$d\vec{l}' = \overline{P'Q'} = \overline{PQ} + \overline{QQ'} - \overline{PP'} = d\vec{l} + \frac{\partial \vec{q}}{\partial l}\, dl dt \tag{18}$$

while the value of $\vec{q}$ corresponding to P' is given by

$$\vec{q}' = \vec{q} + \frac{d\vec{q}}{dt} dt \tag{19}$$

Then, using equations (17), (18) and (19) and omitting a term of highest order, it is found that

$$\Gamma' - \Gamma = \oint \left[\vec{q} \cdot \frac{\partial \vec{q}}{\partial l}\, dl dt + \frac{d\vec{q}}{dt} \cdot d\vec{l} dt + \frac{d\vec{q}}{dt} \cdot \frac{\partial \vec{q}}{\partial l}\, dl\, (dt)^2 \right] = dt \oint \left[\frac{\partial}{\partial l} \left(\frac{q^2}{2} \right) dl + \frac{d\vec{q}}{dt} \cdot d\vec{l} \right] \tag{20}$$

Where the integral is to be extended along C. Equation (20) is still true for any continuously distributed mass. For an inviscid fluid, however, the value of the acceleration vector $\frac{d\vec{q}}{dt}$ may be taken from the equation of motion.

$$\frac{d\vec{q}}{dt} = \vec{F} - \frac{1}{\rho} \operatorname{grad} p$$

where $\vec{F} = -g \operatorname{grad} h$. Moreover, for an elastic fluid the notion of pressure head P/g can be used, giving

$$\frac{1}{\rho} \operatorname{grad} p = \operatorname{grad} P.$$

Thus the expression for $\frac{d\vec{q}}{dt}$ takes the form

$$\frac{d\vec{q}}{dt} = -\text{grad}\,(gh + P) \tag{21}$$

and
$$\frac{d\vec{q}}{dt} \cdot d\vec{l} = -\text{grad}\,(gh + P) \cdot d\vec{l} = -\frac{\partial}{\partial l}(gh + P)\,dl$$

When this is inserted in equation (20), there results

$$\Gamma' - \Gamma = dt \oint \frac{\partial}{\partial l}\left[\frac{q^2}{2} - gh - P\right] dl \tag{22}$$

The quantity within the bracket is a single-valued function of position and time. Thus, since at a given time the integral is extended around the closed curve $\mathbf{C}$, its value is zero. Thus, equation (22) gives $\Gamma' - \Gamma = 0$ or: In an inviscid elastic fluid, the circulation around any closed curve does not change as the particles forming the closed curve move along. This is Kelvin's theorem. The theorem depends essentially on the fact that the equation of motion can be expressed in the form equation (21), i. e., on the fact that in an inviscid elastic fluid the acceleration vector is a gradient, or (since the curl of a gradient vanished identically) that the curl of the acceleration is zero.

<u>Vortex theorems</u>: Starting from Kelvin's theorem, it is easy to derive two theorems on vortex motion which have been proved by Helmholtz. Consider a vortex tube $\mathcal{H}$ of infinitesimal cross section (Figure 40). The particles of $\mathcal{H}$ after time dt still form a tube $\mathcal{H}'$, because no separation of particles can occur; let it be determined whether $\mathcal{H}'$ is still a vortex tube

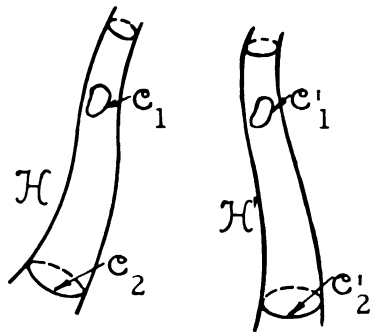

Figure 40. Vortex Filaments Formed by Same Particles

It was found that the circulation must vanish along any closed curve $\mathfrak{C}_1$ lying on the mantle of a vortex tube, but not encircling it. From Kelvin's theorem it follows that the circulation along the new position $\mathfrak{C}'_1$ of this closed curve must also vanish. Also, $\mathfrak{C}_1$ lies on the surface of $\mathcal{H}'$. For an infinitesimal closed curve $\mathfrak{C}'_1$ according to Stokes' theorem, the circulation is the product of the area enclosed within the closed curve by the component of the vortex vector normal to that area. Since this product is zero, the vortex vector must be tangent to the area element at $\mathfrak{C}'_1$, and the closed curve $\mathfrak{C}'_1$ must lie on the mantle of some vortex tube. This is true for any infinitesimal closed curve $\mathfrak{C}_1$ on $\mathcal{H}$ and the corresponding $\mathfrak{C}'_1$ on $\mathcal{H}'$, so that $\mathcal{H}'$ is also a vortex tube of infinitesimal cross section. Thus, the following statement: Particles lying on a vortex line at some moment move in such a way that they form a vortex line at every moment. A shorter expression of this first vortex theorem is: The vortex lines are material lines, in the sense that they always consist of the same particles or material points.

Each vortex tube has a certain vorticity, equal to the circulation along any closed curve encircling the tube, such as $\mathcal{C}_2$ in Figure 40. By Kelvin's theorem, the circulation has the same value along the corresponding closed curve $\mathcal{C}'_2$ on $\mathcal{H}'$, so that the vorticity of the vortex tube $\mathcal{H}'$ is the same as that of $\mathcal{H}$. This gives Helmholtz's second theorem: The vorticity of a vortex tube does not change as its particles move along.

It was seen that vortex tubes cannot come to an end in the interior of the fluid, but must either meet a boundary, extend indefinitely, or be closed. Tubes of the latter type can be observed in air as smoke rings, produced by imparting a rotational motion to the smoke particles. Actually, the smoke rings do not persist indefinitely, in apparent contradiction of the vortex theorems. This is due to the presence of viscosity effects, which are disregarded in the theory of inviscid fluids. The vortex theorems follow from the fact that the acceleration vector is a gradient (and therefore curl-free). To arrive at this statement equation (21) it was necessary to neglect all stress components other than the pressure p (all shearing stresses), and to assume the existence of a relation between p and ρ in order to make possible the definition of P.

Mean rotation and the Bernoulli function: It is known that the total head

$$H = \frac{q^2}{2g} + h + \frac{P}{g} \tag{23}$$

is constant along each streamline during steady flow (Bernoulli equation).

Consider the relation of the Bernoulli function H to the mean rotation of the fluid or to curl $\vec{q}$. Starting from the equation of motion for an inviscid elastic fluid in the form equation (21), subtract grad $\frac{q^2}{2}$ from both sides and use equation (23) to obtain

$$\frac{d\vec{q}}{dt} - \text{grad}\left(\frac{q^2}{2}\right) = -\text{grad}\,(gH) \tag{24}$$

In order to interpret the vector on the left, compute the x-component: Using the Euler rule of differentiation and $q^2 = q_x^2 + q_y^2 + q_z^2$, and denoting briefly curl $\vec{q}$ by $\vec{\Omega}$, it is seen that the x-component of the left-hand side is

$$\begin{aligned}\frac{dq_x}{dt} - \frac{\partial}{\partial x}\left(\frac{q^2}{2}\right) &= \frac{\partial q_x}{\partial t} + q_z\left(\frac{\partial q_x}{\partial z} - \frac{\partial q_z}{\partial x}\right) - q_y\left(\frac{\partial q_y}{\partial x} - \frac{\partial q_x}{\partial y}\right)\\ &= \frac{\partial q_x}{\partial t} + (\Omega_y q_z - \Omega_z q_y) = \frac{\partial q_x}{\partial t} + (\vec{\Omega} \times \vec{q})_x\end{aligned} \tag{25}$$

and from equation (25)

$$\frac{\partial \vec{q}}{\partial t} + (\text{curl}\,\vec{q} \times \vec{q}) = -\text{grad}\,(gH) \tag{26}$$

This (vector) equation (which is a form of Newton's equation for an inviscid fluid), includes the (scalar) Bernoulli equation and more. In fact, for steady flow $\frac{\partial q}{\partial t} = 0$, so that

$$\text{grad}\,H = -\frac{1}{g}(\text{curl}\,\vec{q} \times \vec{q}) \tag{27}$$

Since a vector product is perpendicular to each of its factors equation (27) shows that the vector grad H is perpendicular to $\vec{q}$. Hence the directional derivative of H along a streamline is zero, and H must be constant along the streamline. Moreover, grad H has no component in the direction of curl $\vec{q}$, the direction of the vortex lines. Thus: In the steady flow of an inviscid elastic fluid the surfaces on which the Bernoulli function has constant values are composed of streamlines and vortex lines.

The most important consequence of equation (27) is the following: If curl $\vec{q}$ vanishes at all points, then equation (27) shows that grad $H \equiv 0$, i. e., the Bernoulli function has one and the same value everywhere and therefore: In the steady irrotational flow of an inviscid elastic fluid the Bernoulli function, or the total head, has the same value on all streamlines. The converse is not true in general. It can happen that the streamlines and vortex lines coincide, in which case the vector product curl $\vec{q} \times \vec{q}$ vanishes and H is constant everywhere, although the motion is not irrotational. This case, however, is a very particular type of motion and cannot occur, for example, in a plane motion: $q_z = 0$, $\frac{\partial}{\partial z} = 0$ where equation (13) shows that curl $\vec{q}$ is perpendicular to the x, y-plane and therefore cannot coincide anywhere with $\vec{q}$.

In the case of a non-steady irrotational motion, equation (26) leads to

$$\frac{\partial \vec{q}}{\partial t} = -\text{grad}\,(gH) \tag{28}$$

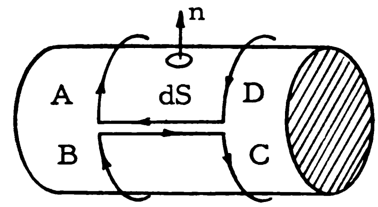

Figure 41. Circulation about Vortex Tube

Vortex Tube: Consider the "circulation" about the vortex tube. Let a portion of tube be as shown in Figure 41, with an imaginary contour A-B-C-D running around and along it. The circulation is

$$\oint \vec{q} \cdot d\vec{r} = \oint_{A-B} \vec{q} \cdot d\vec{r} - \oint_{C-D} \vec{q} \cdot d\vec{r} \tag{29}$$

Stokes' theorem applied to the surface S leads to $\oint \vec{q} \cdot d\bar{r} = \iint_S \vec{n} \cdot (\nabla x \vec{q})\, dS$, so that equation (29) becomes

$$\iint_S \vec{n} \cdot (\nabla x \vec{q})\, dS = \oint_{A-B} \vec{q} \cdot d\vec{r} - \oint_{C-D} \vec{q} \cdot d\vec{r} = \iint_S \vec{n} \cdot \vec{\Omega}\, dS \tag{30}$$

where $\vec{\Omega} = \nabla x \vec{q}$ is the vorticity. Since $\vec{\Omega}$ is a salenodiel field (the divergence of a curl being zero), the last term on the right-hand side of equation (30) is zero by Gauss' theorem, and therefore,

$$\oint_{A-B} \vec{q} \cdot d\vec{r} - \oint_{C-D} \vec{q} \cdot d\vec{r} = 0 \tag{31}$$

or

$$\Gamma_{A-B} = \Gamma_{C-D} \tag{32}$$

Equation (32) states that the circulation about a vortex tube is constant about the length of the tube if the flowing medium is an inviscid fluid. But the flowing medium is not inviscid, and to account for this, the property of constancy of circulation of the flow field is modified in the following manner: instead of considering the vortex filament to be a line without beginning or end in the fluid (Helmholtz's theorem), the filament is assumed to begin in the entrance block (close to station 1) and to end at the exit of the tube. This means that the strength Γ will be a maximum at the entrance, and zero at the exit (the variation, however, is not linear, but is in the manner of Figures 18 and 28). Knowing Γ and its variation, the next step is to calculate the velocity induced by the vortex filament. This is easily done by means of the Biot-Savart law:

$$d\vec{q} = \frac{\Gamma}{4\pi} \frac{d\vec{l} \times \vec{r}}{r^3} \tag{33}$$

or numerically,

$$dq = \frac{\Gamma}{4\pi} \frac{\sin \theta}{r^2} \, dl \tag{34}$$

where θ is the angle made by the position vector and the element of filament dl. Equation (34) can be easily integrated to give the velocity at any point within the vortex tube. Referring to Figure 42 and assuming a rectilinear filament coincidement with the axis of the tube, it is seen that $\sin \theta = \frac{R}{r}$, $r d\theta = dl \sin \theta$. Replacing r and dl in terms of R, $\sin \theta$ and $d\theta$ in equation (34) and integrating gives

$$q = \frac{\Gamma}{4\pi} \frac{1}{R} (\cos \theta_1 - \cos \theta_2) \tag{35}$$

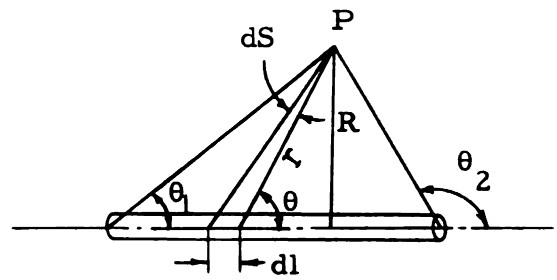

Figure 42. Velocity Induced by Vortex Filament

Equation (35) enables the local velocity to be calculated from the local filament strength and vice versa. In the present case, the velocity is known (from actual measurements) and the strength is calculated. The result is the set of curves in Figures 18 and 28.

As for the viscosity, its influence is seen by writing the equation for the shearing stress in turbulent circular flow:

$$\tau = (\mu + \rho \epsilon)\left(\frac{dq}{dr} - \frac{q}{r}\right) \tag{36}$$

Upon entrance into the tube, the velocity distribution is given by the irrotational relation $q \cdot r = K$, whereupon differentiation gives $qdr + rdq = 0$ or $\frac{dq}{dr} = -\frac{q}{r} = -\frac{K}{r^2}$. Stability considerations, however, require that

$$\frac{dq}{dr} = \frac{q}{r} = \omega \tag{37}$$

This was shown in two previous papers [17, 20] and is tantamount to setting $\left(\frac{dq}{dr} - \frac{q}{r}\right)$ equal to zero. Equation (37) is the condition for rotational or wheel flow (as confirmed by the experimental data). There is, however, another solution to the requirement $\frac{dq}{dr} - \frac{q}{r} = 0$, and this is $\frac{dq}{dr} = \frac{q}{r} = 0$. Physically, it means that the velocity does not change much with respect to r or that it decreases to a negligible value. This is basically what happens near the end of the tube so the analytical treatment just presented does fit rather well with the actual events, in addition to having the merit of mathematical simplicity.

CONCLUSIONS

From the test results gathered over a wide range of entry angles, and from the analytical treatment based on a circulation being induced by a vortex filament coincident with the axis of the tube, the following statement can be made:

1. The vortex effect decreases with the entry angle, but remains significant for entry angles above 45°.
2. The temperature, pressure, and velocity traverse curves at any entry angle have the same general characteristic as those for the 90° (tangential) entry angle.
3. The vortex effect is of small consequence beyond a tube length of nine diameters.
4. The temperature separation depends on the entrance pressure and angle, much less on the entrance temperature.
5. Viscosity first acts to change the flow field from irrotational to rotational (this occurs shortly after inlet and corresponds to the solution $\frac{dq}{dr} = \frac{q}{r} = \omega$).
6. For the remainder of the tube, viscosity acts to alter the wheel flow it first created. This occurs near the end of the tube and corresponds to the solution $\frac{dq}{dr} = \frac{q}{r} = 0$.

BIBLIOGRAPHY

1. Bertin, J., "Modified Hilsch Apparatus for Producing Hot and Cold Air Streams!" (French Patent No. 521, 736, Sept., 1946), Journal of Scientific Instruments, Vol. 28, August, 1951.

2. Bickley, W. G., "Some Exact Solutions of the Equations of Steady Homentropic Flow of an Inviscid Gas," Modern Developments in Fluid Dynamics, Vol. 1, edited by L. Howarth, Oxford at the Clarendon Press,(1953).

3. Binnie, A. M., and Hooker, S. G., "The Radial and Spiral Flow of a Compressible Fluid," Philosophical Magazine, Vol. 23, January-June, 1937.

4. Blaber, M. P., "A Simply Constructed Vortex Tube for Producing Hot and Cold Air Streams," Journal of Scientific Instruments, 27, 168-9, June, 1950.

5. Burkhardt, G., "Theoretical Contribution to the Work of R. Hilsch on the Vortex Tube!' (Translation by R. C. Murray, from Zeitschrift fur Natuforschung, Vol. 3a, No. 1, January, 1948, pp. 46-51, R. A. E. Library), Translation No. 345, June, 1951.

6. Comassar, S. "The Vortex Tube," Journal of American Society of Naval Engineers, 63, 99-108, February, 1951.

7. Deissler, R. G., and Perlmutter, M., "An Analysis of the Energy Separation in Laminar and Turbulent Compressible Vortex Flows," Heat Transfer and Fluid Mechanics Institute, 1958.

8. Curley, W. R., "Report on the Hilsch Vortex Tube," Journal of Boston College Physics Society, May, 1950, pp. 3-9.

9. Eckert, E. R. G., and Harnett, J. P., "Experimental Study of the Velocity and Temperature Distribution in a High Velocity Type Flow," Standard University Heat Transfer Institute Conference, (June, 1956).

10. Einstein, M. A., and L. M., "Steady Vortex Flow in a Real Fluid," Heat Transfer and Fluid Mechanics Institute, Stanford University Press, 1951.

11. Elsler, K., and Koch, M., "Das Verhalten Verschiedener Gase and Die Trennung Von Gasmischen in Einem Wirbelrohr," Zeitschrift fur Naturforschung, 6a, pp. 25-31 (January, 1951), "The Behavior of Various Gases and the Separation of Mixtures of Gases in a Vortex Tube," Translation by G. Coldenwood, R. A. E. Library Translation, No. 400, February, 1952.

12. Fulton, C. D., "Ranque's Tube," Journal of the A. S. R. E., Refrigerating Engineering, 58, 473-9 (May, 1950).

13. Garnick, I. E., and Kaplan, C., "On the Flow of a Compressible Fluid by the Hodograph Method: II - Fundamental Set of Particular Flow Solutions of the Chaplygin Differential Equation," N. A. C. A. Tech. Ref., No. 790 (1944).

14. Hansell, C. W., "Low Temperature Physics," Miscellaneous Developments in German Science and Industry, C-6, Report No. 68, June, 1945, pp. 29-31, The Joint Intelligence Objective Agency, Washington, D. C.

15. Hilsch, R., "Die Expansion Von Gasen im Zentrifugalfeld als Kalteprazess," Zeitschrift fur Naturforschung, Bank I. Heft 4, April, 1946, pp. 208-14. Hilsch, R., "The Use of the Expansion of Gases in a Centrifugal Field in Cooling Process," Review of Scientific Instruments, 18, 2, 108-113 (1947), (unabridged translation).

16. Johnson, A. V., "Quantitative Study of the Hilsch Heat Separator," Canadian Journal of Research, 25, 299,(September, 1947).

17. Kassner, R., and Knoernschild, E., "Friction Laws and Energy Transfer in Circular Flow," Technical Report No. F-TR-2198-ND, GS-USAF Wright-Patterson Air Force Base No. 78 (March, 1948).

18. Knoernschild, E., and Morgenson, "Application of Hilsch Tube to Aircraft and Missiles," AIT33095, Army Air Force, Air Material Command, Engineering Division, Equipment Laboratory, Serial No. MCREXE-664-510A, 45-USAF-Wright-Patterson 128, June 10, 1948.

19. Kreith, F., and Margolis, D.,"Heat Transfer and Friction in Swirling Turbulent Flow," Heat Transfer and Fluid Mechanics Institute, Stanford University Press, 1958.

20. Lay, J. E., "An Experimental and Analytical Study of Vortex-Flow Temperature Separation by Superposition of Spiral and Axial Flows," Parts I and II, Journal of Heat Transfer, Transactions of the A. S. M. E., Series C, August, 1959.

21. Milton, R. M., "Maxwellian Demon at Work," Industrial and Engineering Chemistry (Ind. Ed.), Vol. 38, No. 5, p. 5.

22. Packer, L. S., and Box, N. C., "Vortex-Tube Free Air Thermometry," Cornell Aeronautical Laboratory, Inc., Buffalo, New York, A. S. M. E. Diamond Jubilee Annual Meeting, Chicago, Illinois, Paper No. 55-A-22 (November, 1955).

23. Poritsky, H., "Compressible Flows Obtainable from Two-Dimensional Flows through the Addition of a Constant Normal Velocity," Journal of Applied Mechanics, 13, 1 (March, 1946).

24. Ranque, G. J., "Experiences sur la Detente Giratoire avec Productions Simultanees d'un Echappement d'Air Chaud et d'Air froid." Journal de Physique et le Radium, Suppl. p. 112 (1933). (Translation: G. E. Schnectady Works Library, T. F. 3294).

25. Ranque, G. J., "Method and Apparatus for Obtaining from Fluid under Pressure Two Currents of Fluids at Different Temperatures." United States Patent 1, 952, 281 (March, 1934).

26. Ringelb, F., "Exakte Losungen der Differentialgleichungen einer Adiabatischen Gasstromung," Zeitschrift fur Angewandtle Mathematik und Mechanik 20, 185-198 (1940). Abstract in the Journal of the Royal Aeronautical Society, 46, 403-4-4 (1942), Translation: "Ministry of Aircraft Production," Great Britain, R. T. B. Translation 1609 (1942).

27. Scheper, G. S., Jr., "The Vortex Tube-Internal Flow Data and a Heat Transfer Theory," Refrigerating Engineering, 59, 985-9, October, 1951.

28. Schultz-Grunow, F., "How the Ranque-Hilsch Vortex Tube Operates," Refrigerating Engineering, 59, 52-3 (January, 1951).

29. Sprenger, H., Beobachtungen an Wirbelrohren, "Observation on the Vortex Tube," (Translation by A. O'Donnel from Zeitschrift fur Angewandte Mathematik und Physik, II, 1951, 5, pp. 293-300, R. A. E. Library Translation, No. 394.(December, 1951).

30. Van Deemter, J. J., "On the Theory of the Ranque-Hilsch Cooling Effect," Applied Scientific Research, Netherlands, Sec. A. Vol. 3, 1952, pp. 174-196.

31. Webster, D. S., "An Analysis of the Hilsch Vortex Tube," Journal of the A. S. R. E., Refrigerating Engineering, 58, 163-9; Discussion, 107-71 (February, 1950).

32. Westley, R., "A Bibliography and Survey of the Vortex Tube," The College of Aeronautics Cranfield (1954).

33. Wu, T. Yao-Tsu, "Two Dimensional Sink Flow of a Viscous, Heat Conducting, Compressible Fluid," Quarterly of Applied Mathematics, Vol. XIII, No. 4 (January, 1956).

34. Yeh, H., "Boundary Layer along Annular Walls in a Swirling Flow," Trans. A. S. M. E., Vol. 80, 1958, pp. 767-776.